

AFIT/GE/ENG/96J-01

INVESTIGATION OF RADIO WAVE
PROPAGATION IN THE
MARTIAN IONOSPHERE UTILIZING
HF SOUNDING TECHNIQUES

THESIS

Robert J. Yowell, Civilian, NASA

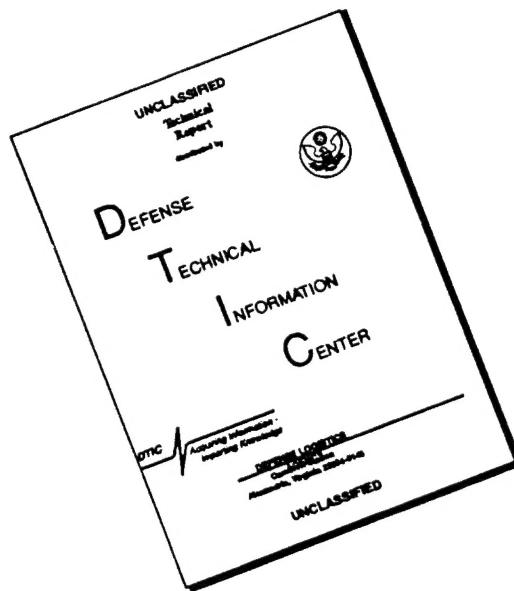
AFIT/GE/ENG/96J-01

19960718 111

Approved for public release; distribution unlimited

DMIC QUALITY INSPECTED 31

DISCLAIMER NOTICE



THIS DOCUMENT IS BEST QUALITY AVAILABLE. THE COPY FURNISHED TO DTIC CONTAINED A SIGNIFICANT NUMBER OF PAGES WHICH DO NOT REPRODUCE LEGIBLY.

**INVESTIGATION OF RADIO WAVE
PROPAGATION IN THE MARTIAN IONOSPHERE
UTILIZING HF SOUNDING TECHNIQUES**

THESIS

Presented to the Faculty of the Graduate School of Engineering

of the Air Force Institute of Technology

Air University

In Partial Fulfillment of the

Requirements for the Degree of

Master of Science

Robert J. Yowell, B. S.

Civilian, National Aeronautics and Space Administration

June, 1996

Acknowledgements

I wish to thank the Johnson Space Center for offering me the graduate fellowship which allowed me to attend AFIT. In addition, I wish to thank my thesis and academic advisor, Major Gerald Gerace, for supporting my work on this thesis, and designing the ed-plan which allowed me to complete my degree within the one year limit of the fellowship.

My late father, Daniel was and will continue to be the source of my inspiration to continue my quest for knowledge. Higher education was always important to my father and to his children; this is forever instilled by the Biblical inscription on his grave which reads: "And those who are wise shall shine like the brightness of the firmament" (Daniel 12:3).

This thesis is dedicated to Daniel and those who will carry the bright flame of knowledge to Mars and beyond.

Table of Contents

Acknowledgments.....	ii
Table of Contents.....	iii
List of Figures.....	vi
Abstract	viii

Investigation of Radio Wave Propagation In The	
Martian Ionosphere Utilizing HF Sounding Techniques.....	1
1.0 Introduction.....	1
2.0 Historical Survey.....	5
2.1 Radio Occultation.....	5
2.2 Nighttime Martian Ionosphere.....	7
2.3 Solar Wind and Cycle Variations.....	9
2.4 Viking Lander Observations.....	10
2.5 Variations Due To Martian Dust Storms.....	12
3.0 Design Approach.....	14
3.1 Specification Requirements.....	15
3.1.1 Launch Vehicle.....	15
3.1.2 Single Probe Carrier.....	15
3.1.3 Multi-Probe Carrier.....	17
3.1.4 Landing Configuration.....	17

3.2	Sounding Theory.....	19
3.2.1	Ionograms.....	22
3.2.2	Chirpsounding.....	26
3.3	Power Supply and Consumption.....	31
3.4	Frequency Selection For Sounder Experiment.....	32
3.5	Antenna Selection For Sounder Experiment.....	33
4.0	Design Implementation	37
4.1	Critical Frequencies	37
4.2	Maximum Usable Frequency	38
4.3	Antenna Design	40
4.4	Horizontal Dipole Antennas	42
4.5	In-Situ Data Transfer	43
4.5.1	Ionogram Sampling Periodicity	44
4.5.2	CLOVER HF Transmission Protocol	45
4.6	Follow-On Experiments	46
6.0	Conclusions and Recommendations.....	49
5.1	Summary	49
5.2	Conclusions	50
5.3	Recommendations	50
5.4	Denouement	51
A	Appendix	53
A.1	Ionospheric Layers	53
A.2	Chapman Layers	54

A.3	Solar Cycle	56
A.4	Martian Ionogram Model	57
B	Bibliography	62
C	Vita	64

List of Figures

1.	Schematic of Mars to Earth Radio Occultation Data Acquisition	7
2.	Electron Density Profiles in the Nighttime Martian Ionosphere	9
3.	Sunspot Number Values During U.S. and Russian Mars Missions	10
4.	Retarding Potential Analyzer Cross Section	11
5.	Electron Density Peaks vs. Solar Zenith Angle During U.S. Mars Missions	13
6.	Single and Multi-Probe Carrier Designs	16
7.	Lander Configuration with Air Bag	18
8.	Lander Entry Profile	18
9.	Oblique Chirpsounder Ionogram	21
10.	Vertical and Oblique Sounding Schematic	22
11.	Simulated Martian Ionogram Using Matlab Software	26
12.	Frequency - Time Representation of Chirp Signals	29
13.	Sample Chirpsounder Ionogram	30

14.	Small Aperture Monopole Antenna	34
15.	Radiation Pattern For Small Aperture Monopole Antenna	34
16.	Small Aperture Dipole Antenna	36
17.	Radiation Pattern For Small Aperture Dipole Antenna	36
18.	Peak Daytime Electron Densities	39
19.	Obliquity Factor	41
20.	Take-off Angles.....	41
21.	Transionospheric Propagation	48
22.	Inverse Transionospheric Propagation	48
A1	Chapman Layer Electron Density Distribution	56

Abstract

This thesis presents a preliminary design of an ionospheric sounder to be carried aboard one or more of NASA's Mars Surveyor landers. Past Russian and American probes have indicated the existence of an ionosphere, but none of these missions remotely sensed this atmospheric layer from the surface. The rationale for utilizing a surface-based Martian ionospheric sounder is discussed. Based on NASA's choice of launch vehicle and power source, a low-weight, low-powered Chirpsounder using a horizontally-polarized dipole antenna is recommended for the sounder experiment. The sounder experiment should be conducted for at least one Martian year, in order to investigate significant changes in radio propagation during seasonal transitions. Specific data compression techniques are suggested in order to reduce the quantity of data transferred from each sounder. The Appendix presents an overview of Earth's ionospheric structure and solar cycle effects. Finally, a Matlab software model of a hypothetical ionogram as measured from the Martian surface is presented.

INVESTIGATION OF RADIO WAVE PROPAGATION IN THE MARTIAN IONOSPHERE UTILIZING HF SOUNDING TECHNIQUES

1.0 Introduction

As of today, humans have set foot on one celestial body beyond Earth, the moon. During six Apollo missions between 1969 and 1972, twelve astronauts walked on the moon, performing scientific experiments with stays lasting up to 3 days. One of the limiting factors involved in these missions for the two astronauts, was the limited range of their UHF (Ultra High Frequency) radio transceivers. With probably the only more vital commodity being oxygen, communication was certainly a necessary life-line for exploration. The moon, lacking an atmosphere, limited communication to line-of-sight operation. This in turn greatly limited the distance in which the astronauts could travel beyond their lunar spacecraft.

In the 21st century, the next great step for human exploration will be landing astronauts on the planet Mars. As we know from several unmanned missions to the 'red planet', Mars not only has an atmosphere, but also an ionosphere. Thus, the Martian environment may allow circumvention of the communications distance limitations of lunar explorers.

Thanks to the radio occultation experiments conducted on the first probes we sent to Mars, we now know that Mars indeed has an ionosphere, albeit one that contains a lower electron density than Earth's. Today, many unknowns still exist regarding the Martian ionosphere, this missing data can only be acquired from the Martian surface.

As the United States and other countries embark on what will be a decade of continuous exploration of the planet Mars, an opportunity exists to further study this planet's ionosphere and prove whether Mars will provide similar conditions that allow the use of terrestrial long distance HF (High Frequency) communications links. One of the missions, the Mars Global Surveyor, along with the European InterMarsnet missions, intends to place several small landers at various points on Mars. These landers will each relay telemetry to an orbiting satellite stationed above Mars, which in turn, will send the data to Earth. In August, 1993, the U.S. Mars Observer spacecraft was catastrophically lost just after entering Mars' orbit. Its onboard communication system was designed as a relay for a future series of unmanned landers. In future Mars lander missions, such a failure of an orbital communication relay would be a tremendous loss, in terms of both dollars and the vast amounts of scientific data that would never be seen on Earth. A relatively inexpensive and practical option exists, which may prove to be a viable back-up system for a future Mars communication satellite relay system. Each of these landers' telemetry streams could be sent separately to one central

lander via HF radio. This central lander would then send the total stream of data to Earth via a standard S-band link.

Long distance HF communication has existed since the beginning of this century. Even with the advent of today's satellite networks linking the globe, ground based HF communications are still used by many governments and commercial enterprises, due to their relative low cost, low power requirements and their simplicity in equipment design.

A simple experiment that could be carried out on two of these landers, using an ionospheric sounder, may verify the feasibility of linking these landers through means of HF radio. This thesis will analyze the design decisions and factors necessary for implementing this experiment.

An ionospheric sounder, or ionosonde deployed on the surface of Mars would provide much greater temporal and spatial measurements of the Martian ionosphere than has been provided by any previous or planned mission. This would lead to a better understanding of the dynamics of the Martian atmosphere, providing valuable scientific knowledge of the processes that controlled the evolution of the Martian environment to its present state.

First, an historical survey will be presented which covers our current knowledge of the Martian ionosphere, and how it was attained through previous U.S. and Russian missions. Next, the design approach for the ionospheric sounder

experiment is discussed, including the specification requirements for the lander itself from Earth launch to Mars landing. The design implementation covers the rationale for selection of power supply, transmit frequencies and antenna selection for the sounder experiment. Following the conclusions and recommendations, an appendix is included which provides an overview of ionospheric morphology and solar cycle phenomena. Finally, the Matlab coding for the Martian ionogram model is presented.

2.0

Historical Survey

The phenomenon of long-range high-frequency radio propagation has been in existence since the turn of the century. Guglielmo Marconi's experiments proved for the first time that radio waves did not necessarily travel in straight lines unless deflected by an obstruction. Following Marconi, scientists such as Heaviside, Chapman, and Appleton established the existence of the atmospheric layer that reflected radio waves, the ionosphere. It is only within the past thirty years that we have discovered the existence of an ionosphere on our neighboring planet, Mars.

A review of the literature pertaining to the Martian ionosphere identifies over a dozen papers, the earliest of which dates back to 1971. The following is a summary of the key topics and papers in this series.

2.1 Radio Occultation Experiments

On July 15, 1965, the U.S. space probe Mariner IV became the first spacecraft to perform a successful fly-by of the planet Mars. One of the main experiments conducted during its mission was a radio occultation measurement (Figure 1). An S-Band tracking signal was transmitted from the spacecraft as it

passed behind the limb of the Martian atmosphere, and again as it emerged. On Earth, the frequency, phase, and strength of the spacecraft's signal was recorded. After analyzing the received signal, the existence of the Martian ionosphere was first confirmed. From changes in phase-path length of the signal and the velocity of its propagation, a measure of the relative electron density in the Martian ionosphere was developed. After Mariner IV, Mariners VI, VII, IX and the Russian Mars 2,3,4, and 5 orbiters provided additional radio occultation data supporting the existence of a Martian ionosphere. Zhang et al. (1990), reanalyzed the Mariner and Viking orbiter radio occultation data. It was concluded that during the daytime, the general behavior of the Martian ionosphere is consistent with that of a classic Chapman layer (See Appendix A.2). Maximum electron concentrations of about $1 - 2 \times 10^5$ electrons / cm^{-3} occur at altitudes from 120 km at the sub-solar point (inferred from the Chapman model) to about 150 km at the terminator. The electron number densities decrease exponentially above the peak, up to the ionopause where the Martian ionosphere interacts with the impinging solar wind. This occurs at a height on the order of 300 - 400 km at the sub-solar point. The ionopause height increases as solar zenith angle decreases.

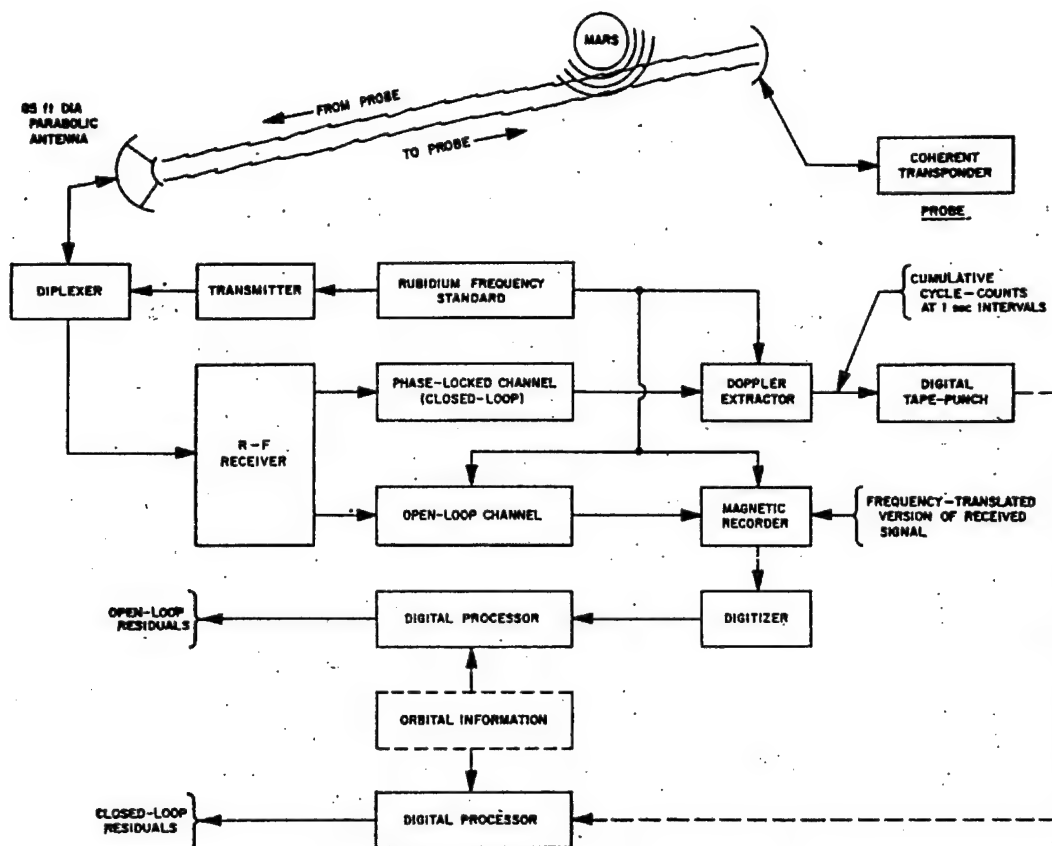


Fig.1—Schematic diagram for occultation data acquisition.

2.2 Nighttime Martian Ionosphere

Radio occultation experiments on the early probes, as well as data from the 1988 Russian Phobos 2 spacecraft provided proof of the existence of an active nighttime Martian ionosphere. The Russian Mars 4 and 5 probes used a method of dual-frequency radio occultation. This form of topside sounding above a dark Martian surface, detected a nighttime ionosphere with an electron concentration of $4.6 \times 10^3 \text{ cm}^{-3}$ for the main peak located at a height of 110 km above the planetary surface (Figure 2). The Phobos 2 spacecraft's magnetometer determined

that the energy of the electrons in the ionosphere is sufficient for the impact ionization of the planetary neutral gas. Also, the characteristic flux of electrons ($\sim 10^8 \text{ cm}^{-2} \text{ s}^{-1}$) could produce the nightside ionospheric layer with a peak density of a few thousands of electrons per cubic centimeter. This data was supported by the conclusion that the Martian magnetic field is induced in the planetary magnetotail and the variability of the nightside ionosphere may be explained by the partial screening of the atmosphere by a weak intrinsic magnetic field of the planet.

The Martian ionosphere often does not completely disappear at night, and electron densities sometimes remain above 10^3 cm^{-3} for solar zenith angles up to 125° . Two possible sources of nighttime ionization are: 1) nightward flow of dayside ions, and 2) precipitating electrons driven by the solar wind interaction with the Martian ionosphere (Zhang et al. 1990). Verigin et al. (1991), using the electron spectrometer observations from the Phobos 2 spacecraft's HARP (Hyperbolic Retarding Potential Analyzer) experiment, found electron energies and fluxes at higher altitudes sufficient to cause impact ionization of CO_2 in the nighttime neutral atmosphere.

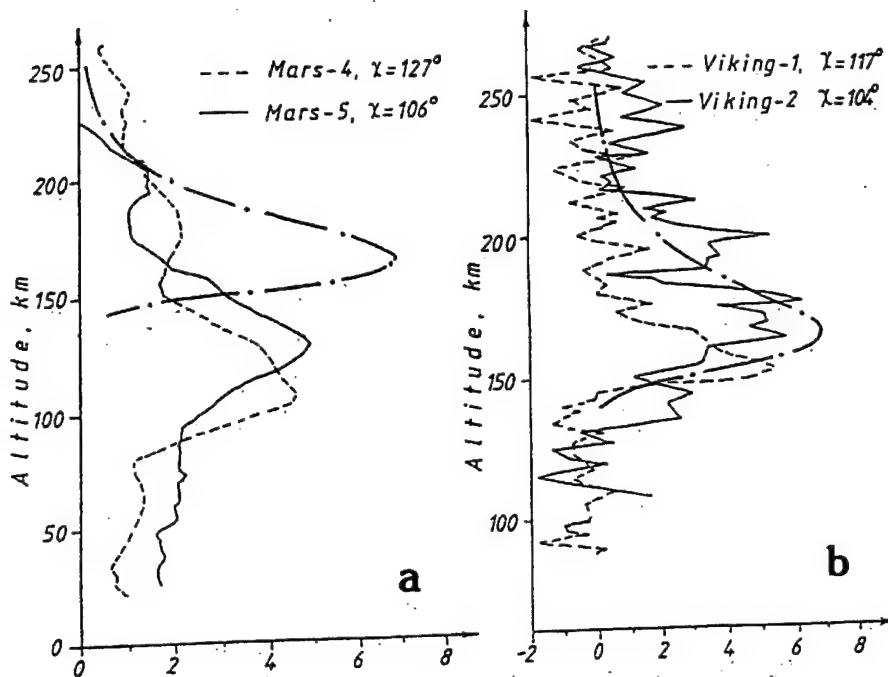


Figure 2 - Plots of altitude vs. electron density (10^3 cm^{-3}) in the Martian nighttime ionosphere from radio occultation measurements of Mars 4 and 5 (USSR) and Vikings 1 and 2 (USA) spacecraft. Dot - dashed line is the data from the Phobos 2 HARP instrument. (Verigin et al., 1991).

2.3 Solar Wind Interaction and Solar Cycle Variations

Since both Russian and US probes have visited Mars during various levels of solar activity, detailed re-analysis of radio occultation data now shows that the Martian ionosphere cannot be described by a simple Chapman layer since the neutral gas scale height and the ionizing radiation fluxes are not constant but variable with solar activity (Fox et al.). In fact, the scale height of the topside Martian atmosphere is unusually sensitive to the variations of solar activity. Another reason for departures from a Chapman-type behavior lies in the fact that the ionizable constituent CO_2 also varies with solar zenith angle.

Figure 3 is a graph of the sunspot cycles from 1950 to 2000, superimposed with the dates of each successful U.S. and Russian Mars mission. Only Mariners 6 and 7 made observations during solar maximum conditions. The Mariner 9 and Viking missions, from which most Martian ionospheric data were obtained, occurred at the time of sunspot minimums in cycle 20.

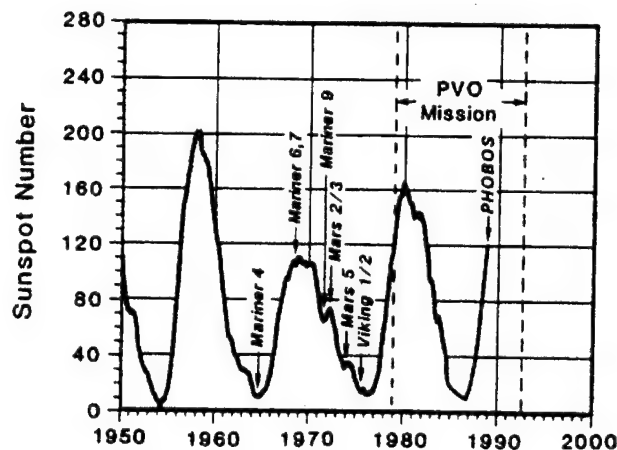


Figure 3 - Sunspot number values during the dates of arrival of Russian and American Mars spacecraft. (Verigin et al., 1991).

2.4 Viking Lander Observations

In July, 1976 the Viking 1 lander became the first spacecraft to make in-situ measurements of the ionosphere of another planet (Chen et al. 1978). During its descent to the Martian surface, the lander took detailed measurements of the ionosphere with an instrument known as an RPA (Retarding Potential Analyzer). In 1988, the Russian spacecraft, Phobos, carried the HARP RPA. This instrument, commonly used on Earth orbiting scientific satellites, determines ion

concentrations by “collecting” them on a probe (Hargreaves, 1992). By projecting the probe out in the ionosphere, an electric current of electrons or in some cases, ions are drawn into the probe. A trap collects ions from the medium because the spacecraft is moving faster than the ions. Grids in the trap act as screens, keeping out electrons or screening the detector from electrical changes on other grids (Figure 2). The G2 grid has a potential that is varied between 0 and +32 V. Most ions will arrive with approximately the same velocity (the speed of the spacecraft), but the G2 grid will reject the lighter ones. Thus the ion concentration is determined for the various masses present, and ion temperature can be deduced from the current-voltage curve.

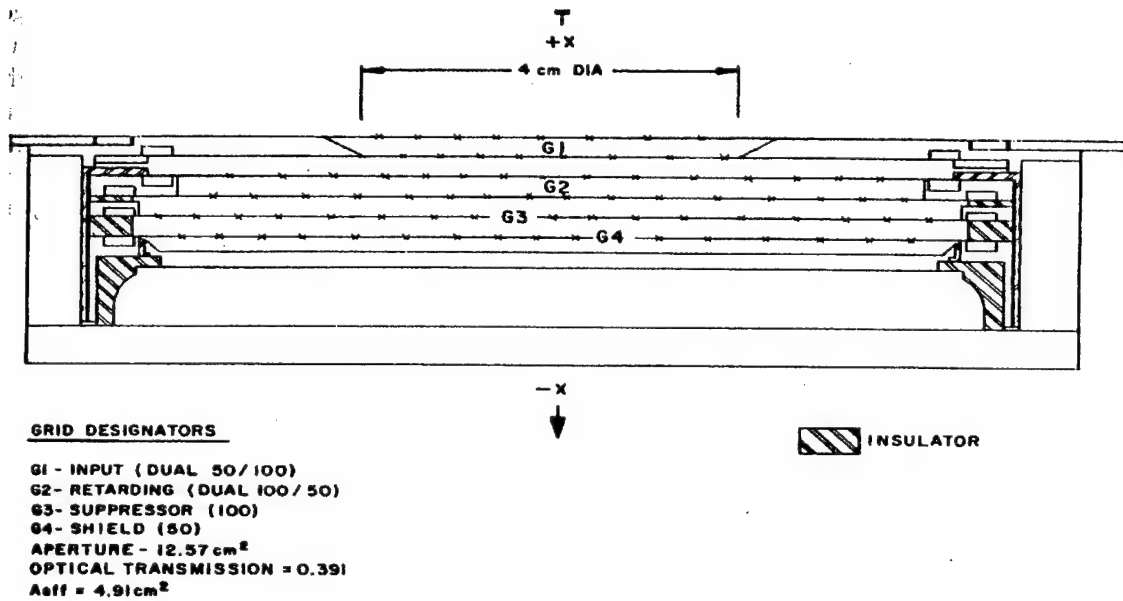


Figure 4 - Retarding Potential Analyzer Cross Section. (Hargreaves, 1992)

2.5 Variations Due To Martian Dust Storms

One of the most intriguing results returned from the Mariner 9 radio occultation data in 1971 was a noticeable effect of a Martian dust storm on the Martian ionosphere. As luck would have it, Mariner 9 arrived at Mars during a major dust storm, thereby hampering its ability to take a detailed photographic survey of the planet's surface, but provided additional time for radio occultation measurements. The altitude of the electron density peak rose by over 20 km than its level measured during nominal atmospheric conditions (Figure 5). Some have explained this effect due to upper atmospheric temperature and density modifications caused by dust activity at lower altitudes. This phenomenon though, is still not completely understood, and presents an excellent opportunity for future experiments. One such experiment would be to determine whether such a dust storm may produce a sporadic-E type effect on Mars. On Earth, sporadic-E propagation usually occurs during temperature-inversion periods in the summer season, or due to meteor showers. On Mars, the high levels of dust in the lower atmosphere may produce an inversion-like effect in the upper atmosphere.

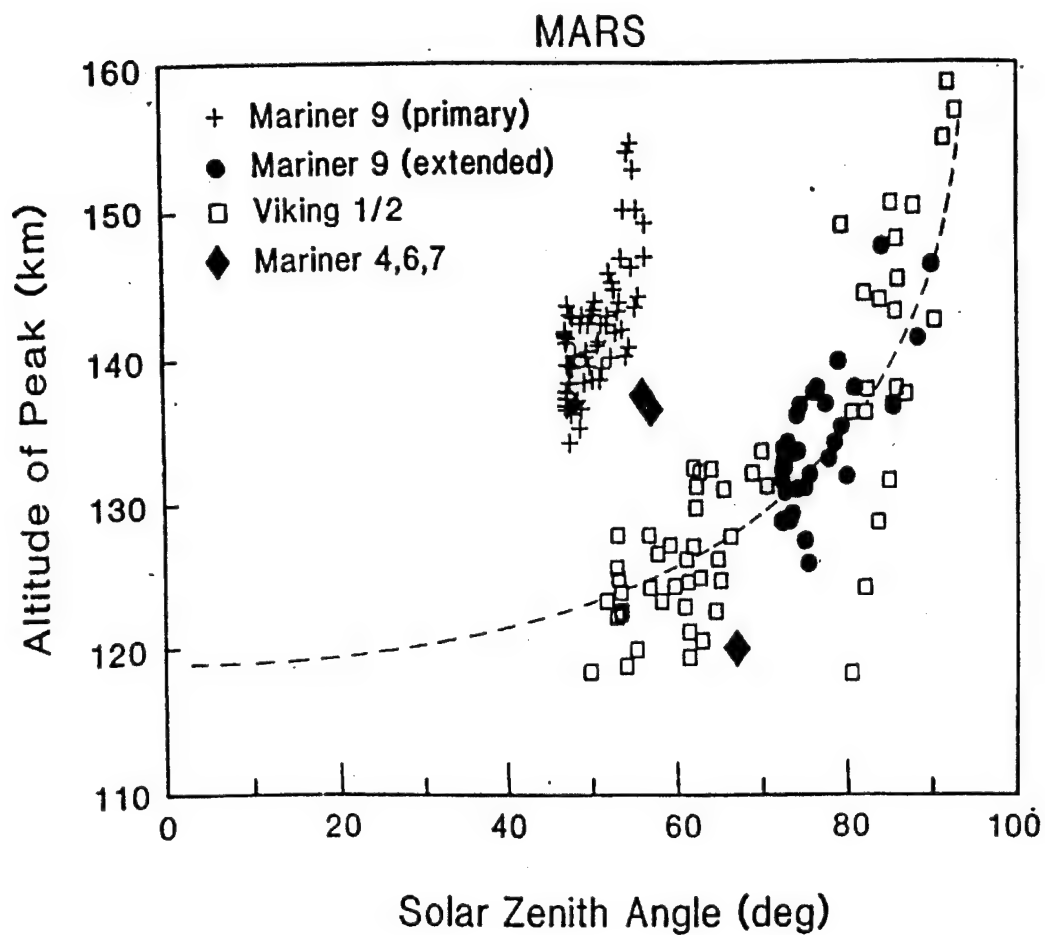


Figure 5 - Altitudes of measured electron density peaks vs. solar zenith angle during U.S. Mars missions. Note the anomalous high peak during the large dust storm of 1971 at the time of Mariner 9's arrival. (Luhmann, 1995).

3.0 Design Approach

This section will propose a relatively low power, low weight ionospheric sounder that may be 'piggybacked' on an unmanned Mars lander. The purpose of the experiment will be to characterize in detail, whether the Martian ionosphere has the potential for propagating RF signals at long distances. This data will also provide valuable scientific data by detailing for the first time how the bottom-side Martian ionosphere varies with Martian seasons, dust storms and solar cycle activity (See Appendix A.3); important factors which in turn may allow us to better understand our own terrestrial atmosphere. In addition, this data will dramatically increase our knowledge of the morphology and evolution of the Martian atmosphere.

In keeping with the spirit of NASA's "faster, cheaper, better" philosophy, the Martian ionospheric sounder will be optimized for size, power consumption and weight. This will allow it to be prime candidate for flight aboard the Mars Surveyor class of unmanned landers.

3.1 Specification Requirements

3.1.1 Launch Vehicle

The type of launch vehicle and the carrier is a major driver with respect to the specification requirements of the lander itself. For the "Discoverer" class of missions that both Mars Surveyor and InterMarsnet belong to, the launch vehicle is a Delta II 7925 expendable rocket. This booster would allow for a 1000 kg maximum launch weight to Mars, delivering three or four landers to the surface, and leads to a target mass of 120 kg per lander.

The "carrier" or platform that will house the landers on the way to Mars can be designed to carry either a single lander or multiple landers.

3.1.2 Single Probe Carrier

By using three separate single-probe carriers in the Delta launch vehicle, the maneuvers during cruise and approach phases are simplified, and the entry and targeting accuracy is improved. A down-side is that the ground has to now manage three separate free-flying spacecraft. For a power supply, use of

solar arrays on both the carrier and probes would be inefficient, since the solar array for the carrier would require a very large area. The only alternative would be to use 2 RTG's (Radioisotope Thermal Generator), one on the lander and one on the carrier, with the two coupled during launch and approach phases. Such a complex power supply would lead to thermal and radiation problems. For mass and cost effectiveness, the single-probe carrier concept must also be designed to utilize to the maximum extent all lander subsystems: command and data management, power supply and thermal conditioning. This not only de-optimizes the mass and power related design characteristics of the lander subsystems, it also complicates the overall design, since multiple carriers will be launched. The Delta II's nose fairing volume limits the number of single carriers in one launch to three. For these reasons, a single probe carrier is not a good option. These limitations may be overcome through the use of a multi-probe carrier. Figure 6 shows the single and multi-probe carrier configurations.

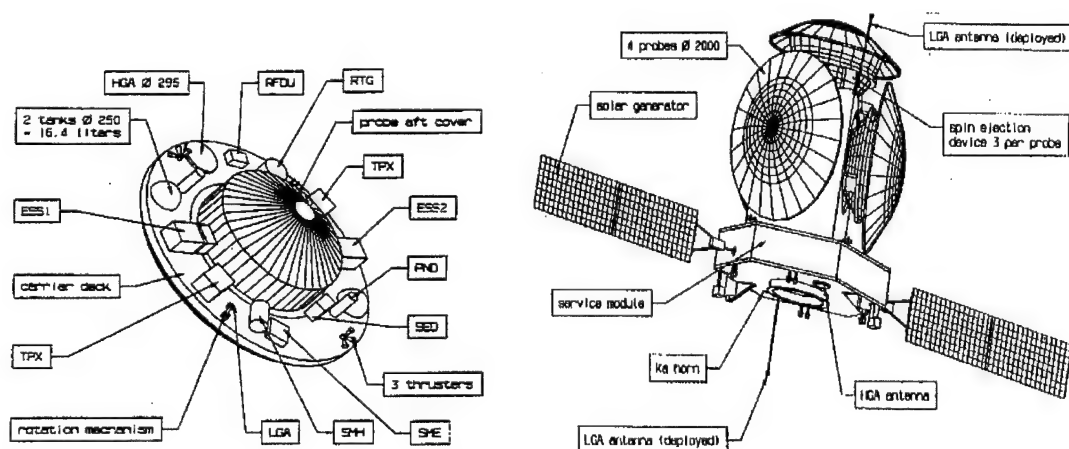


Figure 6 - Single and Multi-probe carrier designs for Mars Surveyor/InterMarsnet. (Chicarro, 1993)

3.1.3 Multi-Probe Carrier

The multi-probe carrier concept provides several advantages over the single probe concept. Most notably, the multi-probe carrier reduces the amount of spacecraft that ground control must manage during cruise and coast from three to one. In addition, the multi-probe carrier allows the carrier and probe subsystems to be completely de-coupled and optimized separately. In addition, the individual solar arrays on each probe may be coupled during the cruise phase to provide the necessary power supply. The Delta II launch fairing allows the accommodation of a multi-probe carrier with four landers.

3.1.4 Landing Configuration

The individual landing probes will enter the Martian atmosphere at a velocity of 6.3 km/s. A descent subsystem consisting of a drogue and main parachute will provide stabilization of the lander through supersonic, transonic and subsonic flight, reducing the lander's vertical impact velocity to 20-30 m/sec. Figure 7 illustrates the air-bag that will deploy 850 meters above the landing surface. Figure 8 illustrates the entire approach and entry profile.

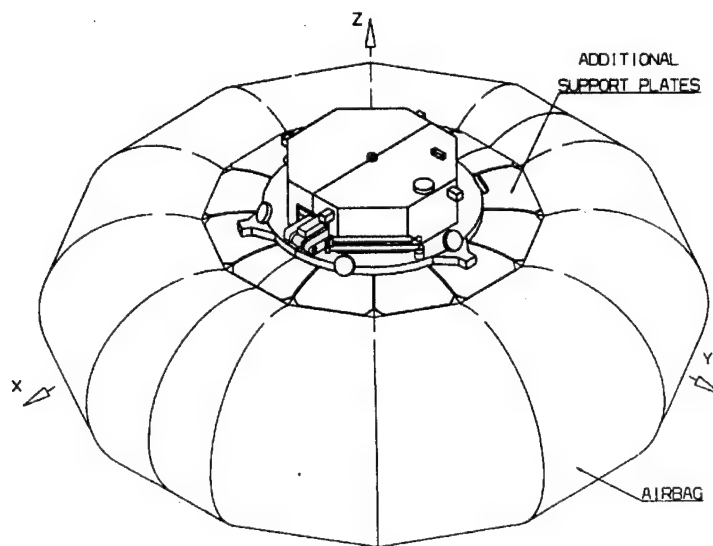


Figure 7 - Lander configuration with deployed air-bag. (Chicarro, 1993)

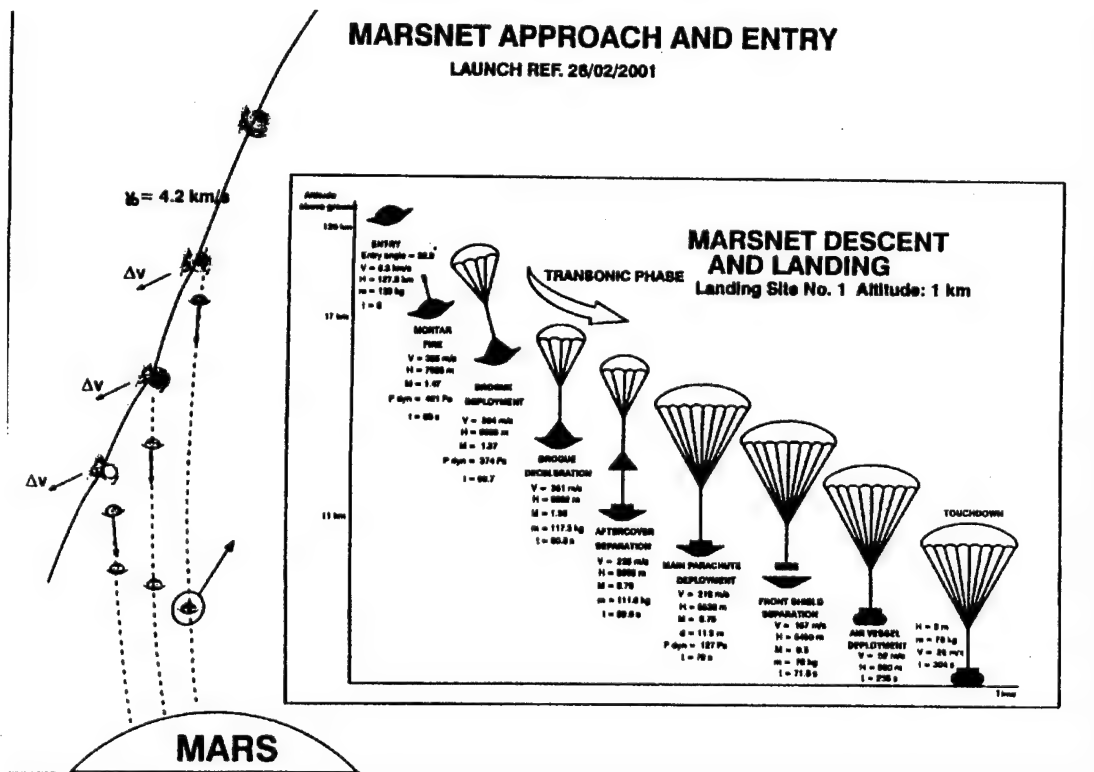


Figure 8 - Lander Entry Profile (Chicarro, 1993)

3.2

Sounding Theory

The technique of vertical ionospheric sounding permits measurement of the travel time a radio pulse moves between the ground and its reflected point in the ionosphere. A pulse transmitter and receiver are synchronously swept in frequency. The 'echo' delay time is then recorded as a function of the radio frequency. This recorded data is known as an 'ionogram' and an example is shown in Figure 13. In practice, this 'echo' delay time is replaced by a virtual height in the ionogram. This assumes that the radio wave propagates at the speed of light, which of course is not the case. The refractive index of the plasma must be taken into account.

In the presence of a magnetic field, the ionosphere is a double refracting medium, creating two possible modes of wave propagation. The refractive index is :

$$n^2 = 1 - \frac{X}{1 \pm Y} \quad (1)$$

where $X = \omega_N^2 / \omega^2$ and $Y = \omega_H / \omega$, ω is the radio wave frequency, ω_N is the plasma frequency which is given by $(N_e e^2 / m \epsilon_0)^{1/2}$, and ω_H is the electron gyro frequency given by eB/m . In these expressions of characteristic frequencies, N_e is the electron density, ϵ_0 is the permittivity of free space, e and m are the electron charge and mass respectively, and B is the magnetic field. In equation

(1), the sign “+” refers to the ordinary wave, or O mode, and the “-” sign refers to the extraordinary wave, or X mode. When the frequency increases during the sweep, the ordinary wave is reflected at the level where $X=1$ (if $\omega_N > \omega$, the refractive index is imaginary and the wave cannot propagate), and the extraordinary wave is reflected at the level where $X = 1 - Y$. Thus, the characteristic frequency of the O mode is:

$$\omega_0 = \omega_N \quad (2)$$

the characteristic frequency of the X mode is:

$$\omega_X = 1/2 \left[\omega_H + (4\omega_N^2 + \omega_H^2)^{1/2} \right] \quad (3)$$

and the traces of the ordinary and extraordinary waves are seen in Figure 9. The vertical electron distribution can be obtained through an inversion technique. For a weak magnetic field ($\omega_C \ll \omega_N$), the critical frequencies of the O and X modes are related by:

$$\omega_O = \omega_X - \omega_H/2 \quad (4)$$

Thus the difference between these two characteristics is directly related to the value of the magnetic field. In the absence of a magnetic field, which is believed to be the case on Mars, the ordinary mode is the only significant one that would be present.

There are two major types of sounding techniques - Vertically incident(VI) and obliquely incident (OI) . VI ionograms are used for studying the overall structure and electron density levels of the ionosphere, but no propagation data is obtained. A major advantage of VI sounding is that the transmitter and receiver are co-located, providing ease of data collection and reduced cost. An OI ionogram is useful for observing propagation conditions. This is possible because unlike the VI sounder, the OI requires a separate receiver and transmitter (Figure 10).

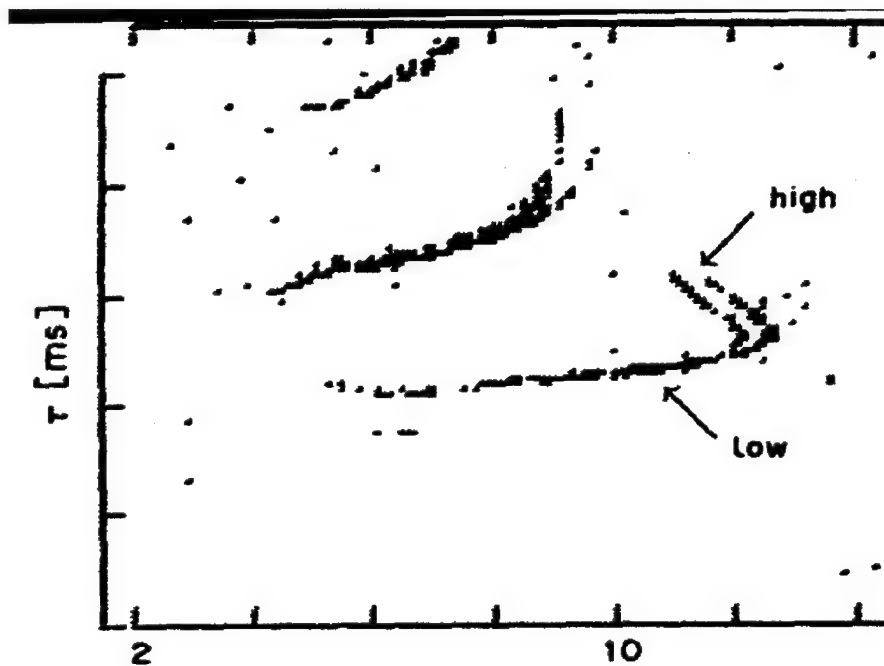


Figure 9 - Oblique ionogram using a Chirpsounder (x-axis is freq. in MHz)

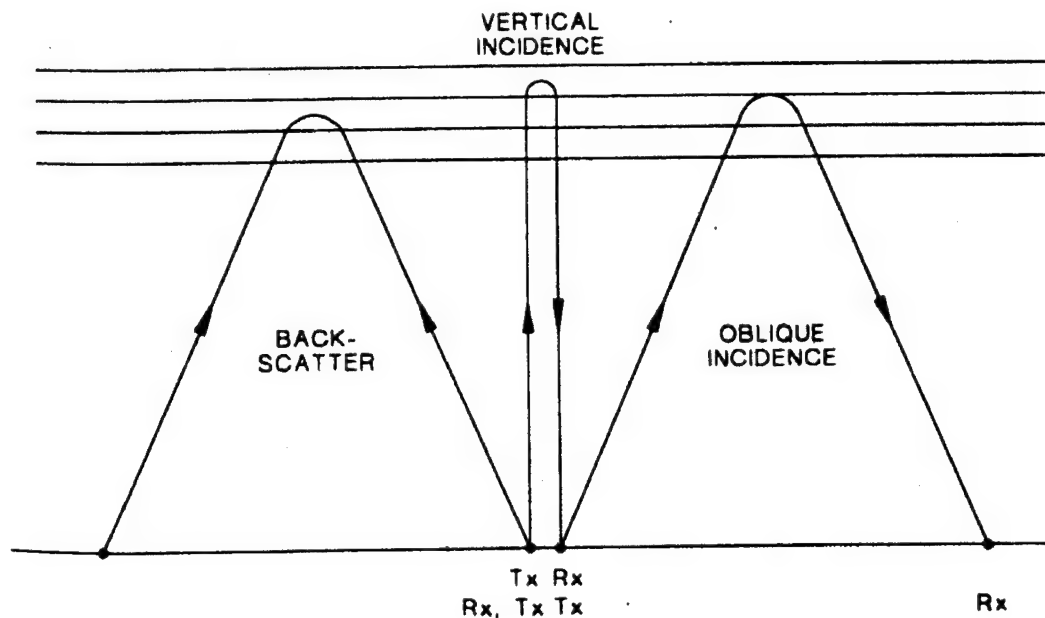


Figure 10 - Schematic of vertical and oblique sounding (McNamara, 1991)

3.2.1 Ionograms

An ionogram is a plot of the apparent, or virtual length of a propagation path as a function of frequency. The plot is generated from the sounder, or ionosonde, which transmits radio wave energy from a swept-frequency transmitter and received by a receiver. The ionograms generated from VI sounders give a direct representation of the critical frequency of the ionosphere. This is done by measuring the time delay for the RF energy to return to the receiver and converting this into the virtual height, from which the signal was reflected.

To calculate the ionogram, we consider the pulse of radio energy being transmitted vertically by the transmitter, reflected by the ionosphere, and returning

to the receiver a time T later. The group, or virtual height, h' at a specific radio frequency is the distance that a radio wave traveled in half the elapsed time, $T/2$ if it had traveled at the speed of light in free space (c). Thus,

$$h' \equiv c T / 2 \quad (5)$$

The velocity at which the energy of the signal travels, v , is related to the speed of light by:

$$v = c / \mu' \quad (6)$$

where μ' is the group refractive index. Since $dh/dt = v$ this yields:

$$h' = \int_0^{hr} \mu' dh \quad (7)$$

where the integration limits are $h=0$ (the surface) and $h=h_r$, the reflection height.

Since $\mu' = 1$ in the free space below the base of the ionosphere, h_0 , this can be written as:

$$h' = h_0 + \int_{h_0}^{hr} \mu' dh \quad (8)$$

where the lower limit is h_0 . For the case of no magnetic field and no collisions (like Mars), the phase refractive index, μ for a radio frequency f , and a plasma frequency, f_N gives:

$$\mu^2 = 1 - (f_N/f)^2 \quad (9)$$

Because the refraction index is a function of the plasma frequency, this yields the following for virtual height:

$$h' = h_0 + \int_0^f \mu'(f_N) \cdot (dh/df_N) df_N \quad (10)$$

the limits for the integral are from $f_N = 0$ to $f_N = f$ where f is the radio frequency.

This integral yields an infinite result for h' when the gradient of the plasma frequency, $df_N / dh = 0$, which occurs at the peak of the ionospheric layer. This is solved by changing the variable of integration from f_N to X , ($X = f_N^2 / f^2$), ($f_N = (f^2 X)^{1/2} = f \cdot X^{1/2}$), thus

$$h' = h_0 + \int_0^1 \mu'(X)(dh/df_N)(f^2/2f_N) dX \quad (11)$$

with the limits of integration as $X = 0$ and $X = 1$. And this yields:

$$h' = h_0 + \int_0^1 1/(1-X)^{1/2} dh/df_N f^2/2f_N dX \quad (12)$$

We can solve this equation analytically and produce a final linear equation which defines the parabolic trace of the ionogram. We start by defining the fundamental relationship of the plasma frequency, $f_N = (80.5 Ne)^{1/2}$. The electron density Ne , can be defined as a linear function: $ne = \alpha h + \beta$. Thus, the plasma frequency expression becomes: $f_N = (80.5(\alpha h + \beta))^{1/2}$. Using the expressions derived above, we now have the fraction df_N/dh equal to: $1/2(80.5(\alpha h + \beta))^{-1/2} (\alpha \cdot 80.5)$. The

expression for X now becomes: $80.5 (\alpha h + \beta) / f^2$. Finally, substituting this expression in equation 12 yields:

$$h' = h_0 + \int_0^1 1/(1-X)^{1/2} \alpha(80.5) f^2 dX \quad (13)$$

this simplifies to:

$$h' = h_0 + \alpha (80.5) f^2 \int_0^1 1/(1-X)^{1/2} dX \quad (14)$$

Finally, solving the integral yields:

$$h' = h_0 + \alpha (80.5) \bullet 2f^2 \quad (15)$$

A simulated ionogram can be obtained by evaluating equation 15 at different radio frequencies. Figure 11 shows a simulated Martian ionogram, evaluated in this manner. According to this model, the critical frequency of the Martian ionosphere is approximately 2 MHz. See Appendix A.4 for more details regarding this software model.

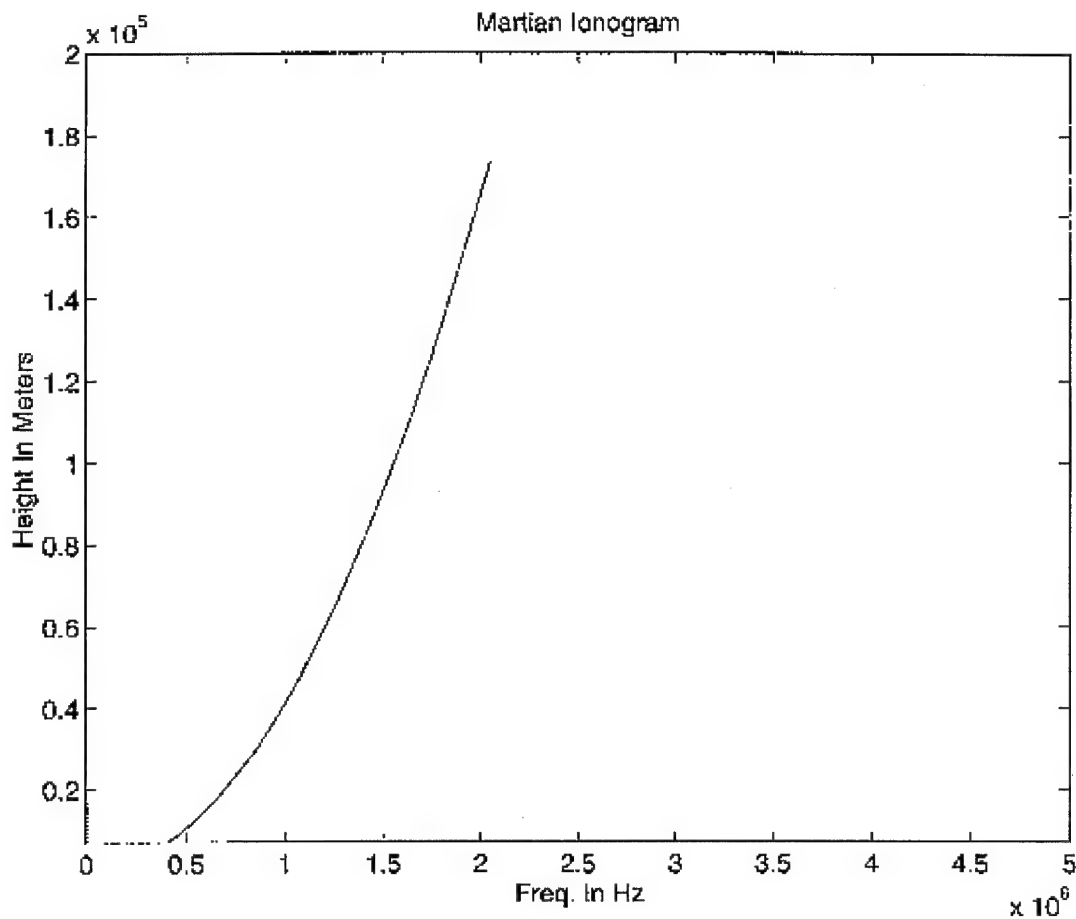


Figure 11 - Simulated daytime Martian ionogram using Matlab software

3.2.2 Chirpsounding

In contrast to pulsed sounding, one can use an FM (Frequency Modulation) technique known as Chirpsounding. The Chirpsounder is a receiver that sweeps through the HF spectrum at a fixed rate, synchronized with a transmitter either co-located (VI sounding), or located at the other end of an HF

link (OI sounding). The principle of operation is that the frequency of the transmitted signal varies linearly in time with slope (Figure 12).

The transmitter emits an FM (frequency modulated), CW (continuous wave) signal that starts at a given time and frequency with a pre-determined sweep rate. An internal clock in the receiver starts the sweep of the receiver local oscillator synchronously with the transmitter, with a fixed frequency offset. The receiver's local oscillator is tuned to a slightly higher frequency than the transmit frequency in order to place the receive signal in a convenient passband. The time elapsed during the travel of the RF signal from the transmitter via the ionosphere to the receiver causes the received signal to have a delay-dependent frequency lag relative to the instantaneous frequency of the receiver's local oscillator (Davies, 1990).

The Chirpsounder benefits from the noise discrimination characteristic of FM. This is not the case with the echo recognition algorithms of pulse ionosondes, where noise can become a negative factor. An echo from a Chirpsounder is actually an impulse in frequency rather than the time domain. In the frequency domain an impulse due to noise is statistically unlikely, and thus echoes are easily distinguished from noise through the use of a reference amplitude margin which a random impulse is unlikely to exceed. This can be clearly demonstrated during a thunderstorm on Earth while listening to the radio.

One does not hear static crashes on FM frequencies, but they are very prevalent on AM frequencies.

Each ionospheric echo can be expressed in terms of five parameters as a multidimensional variable E as follows:

$$E = E(R', V^*, \theta_{NS}, \theta_{EW}, P)$$

where

$R' (f,t)$ = group slant range

$V^* (f,t)$ = phase, or Doppler velocity

$\theta_{NS} (f,t)$ = arrival angle in north-south direction

$\theta_{EW} (f,t)$ = arrival angle in east-west direction

$P (f,t)$ = echo amplitude

$f_o(t)$ = sounding frequency

t = time

Figure 13 shows a collection of discrete values of the echo variable E for an experiment where the sounding start frequency f_o varied linearly.

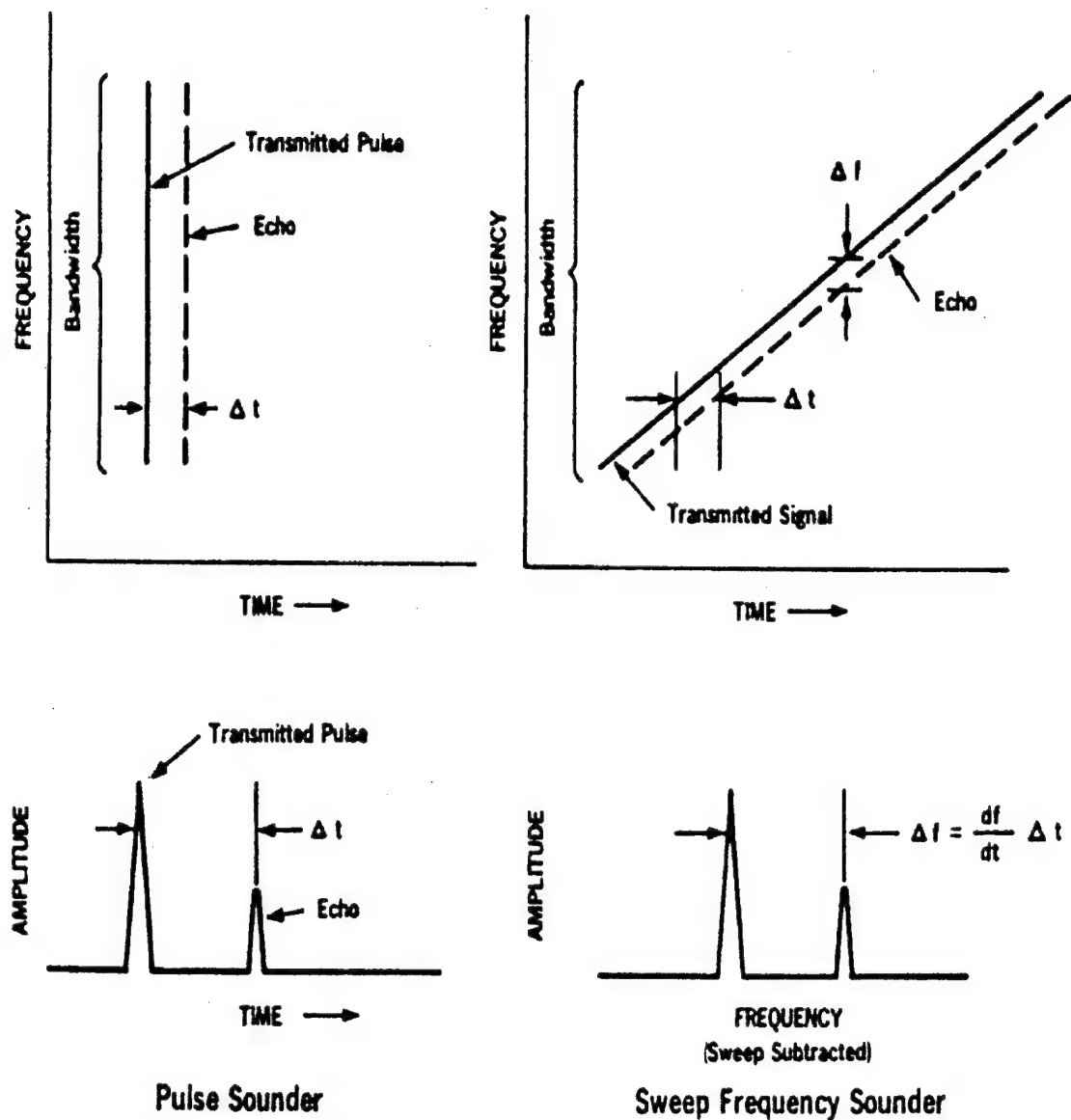


Figure 12 - Frequency-time representation of pulse sounder signals (left), and frequency-modulated continuous wave signals of a Chirpsounder (right) (Davies, 1990)

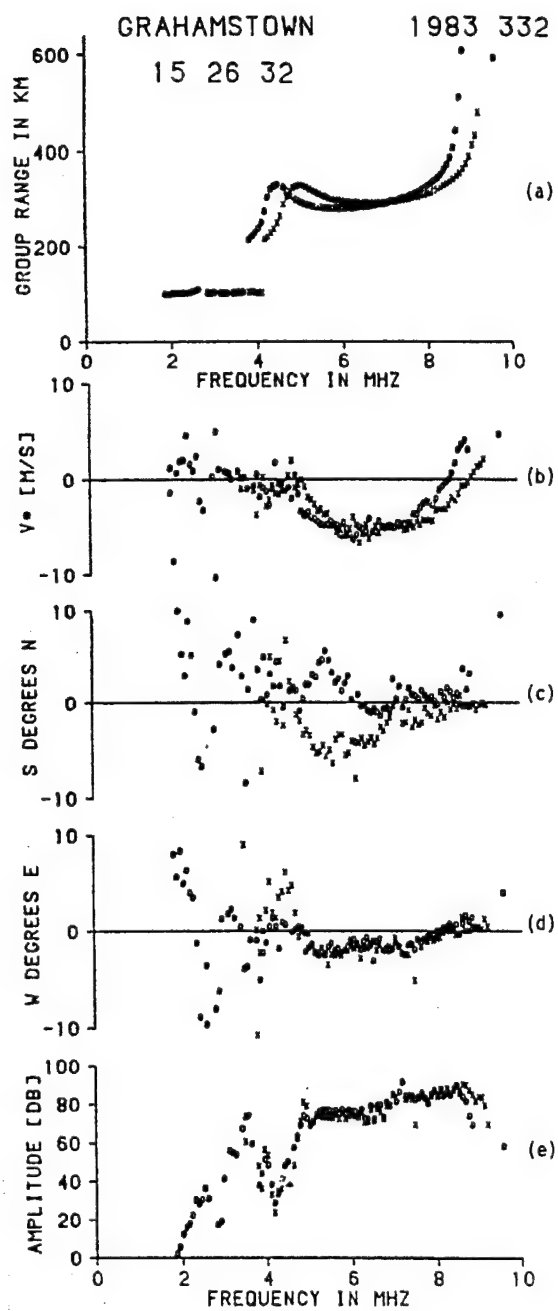


Figure 13 - Sample Chirpsounder ionogram taken at Grahamstown, South Africa. (Davies, 1990) Graph Description: a) Group height (R'), b) Doppler velocity (V^*), c) Arrival angles in north-south direction (θ_{NS}), d) Arrival angles in east-west direction (θ_{EW}), e) Echo amplitude (P).

3.3 Power Supply and Consumption

For the purpose of low cost, simplicity of design, and planetary protection, a solar array design for each lander will be used, vice an RTG. The location of each landing site (between $+40^{\circ}$ N and -40° S Martian latitudes) will limit the amount of power available for experiments and spacecraft subsystems. Low solar constant at Mars, long nights, and the potential for dust storms will require payload and subsystem power consumption to be extremely rationed.

The lander solar array will have an octagonal shape, matching the structure of the top surface structure. It consists of 6 vertical and rectangular panels and 8 horizontal and trapezoidal panels, covering an area of 1.38 m^2 in silicon cells. The maximum power generated by this array is 300 W DC at maximum solar charge. At night, a lithium battery of maximum 7 amps/hr of current will be utilized. Table 1 shows the total lander power budget based on 5 Mbit/day of data transmission to Earth. The majority of this data is from the seismometer (3 Mbit). The meteorological package transmits 1 Mbit, while the other 1 Mbit comes from lander housekeeping data (thermal, power, and overall systems status).

LANDER POWER BUDGET									
Subsystem	Daytime			Night (battery)			Peak (battery)		
	W	h	Wh	W	h	Wh	W	h	Wh
Payload			5.14			9.76			
SEM	0.55	8.5	4.68	0.55	16.00	8.80			
MEP	0.06	8.5	0.47	0.06	16.00	0.96			
CDMS	0.22	8.5	1.83	0.22	16.00	3.44			
Comm.							17.5	0.43	7.53
P.C.			4.62			8.73			6.88
Harness			0.12			0.22			0.23
Subtotal			11.71			22.15			22.92
Battery req. energy									45.1
Battery charging						50.07			
SA req. power									61.8

Day: 24.5 h; daytime minimum: 8.5 h; nighttime maximum: 16 h; battery charge: 8 h; charge ratio: 0.9.

Table 1 - Lander power budget for the InterMarsnet lander. (Chicarro, 1993)

(SEM = Seismic Equipment Module), (MEP = Meteorologic Experiment Package), (CDMS = Command and Data Management System)

An ionospheric sounder should add only 10-15 W of input power to this profile in order to preserve the existing power budget. It is important we select a sounder with a sensitive receiver to overcome the limitations of a low powered transmit signal. More importantly, the choice of antenna will greatly improve the chances of successful operation with minimum input power.

3.4 Frequency Selection for Sounder Experiment

Based on our current knowledge of the Martian ionosphere's electron density profile, as well as the performance of terrestrial based ionosondes, we can ascertain within +/- 10 MHz, the optimal range of frequencies one would use

for over the horizon communications on Mars. This range is slightly below that of Earth-based ionosondes, which operate in the range of 2 to 30 MHz.

Therefore, it is proposed that the first sounding session on the Martian surface be conducted over as broad a range of frequencies as possible. After this has completed, the sounder will be remotely commanded to reduce the set of sounding frequencies to those that lie within the received spectrum from the initial sounding. This first "sweep" will be from 0.5 to 20 MHz.

3.5 Antenna Selection for Sounder Experiment

For the ionospheric sounder, antenna selection is driven mainly by size, ease of deployment, robustness of design, and most importantly, gain.

Since the sounder will be operating in both a vertically incident (VI) and obliquely incident (OI) mode, antennas of both a vertical and horizontally polarized variety will be utilized. Figure 14 shows a small aperture monopole antenna. This antenna is optimized for a vertical polarization of RF radiation. It is omnidirectional, and has an overall height of 203 cm. The radiation pattern is shown in Figure 15.

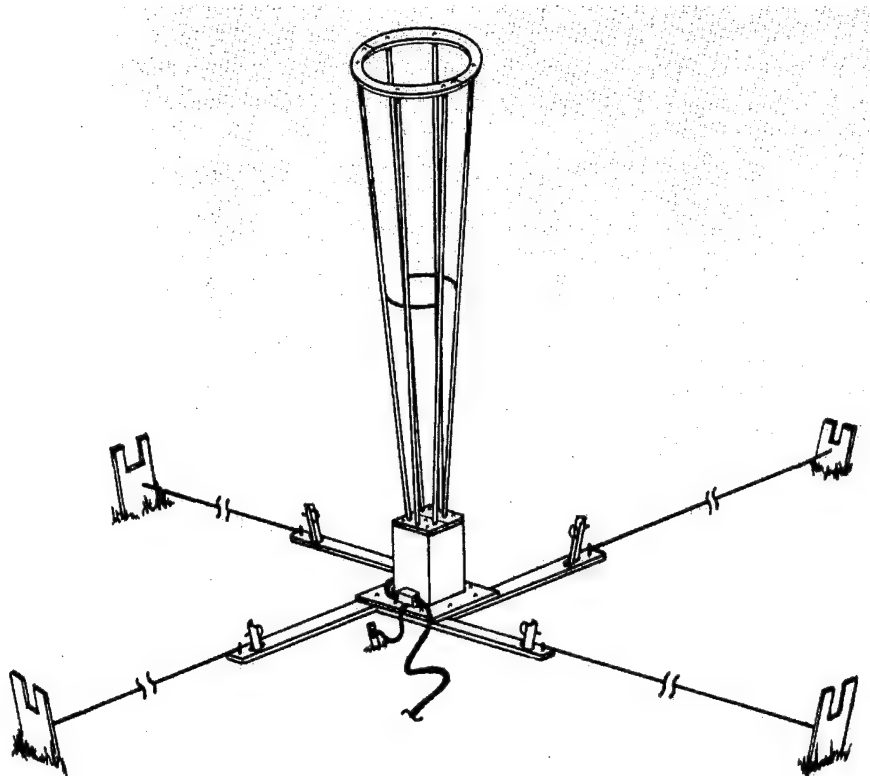
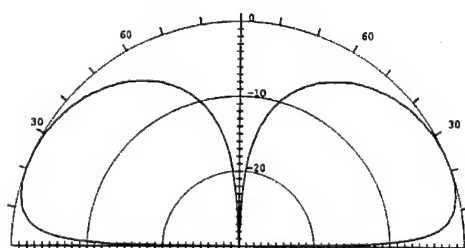
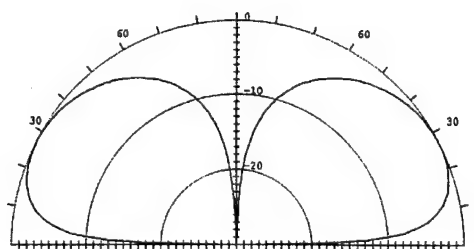


Figure 14 - Small Aperture Monopole Antenna - (Harris Corporation)



RF-1955 Elevation Pattern for Average Soil Characteristics at 2 MHz



RF-1955 Elevation Pattern for Average Soil Characteristics at 30 MHz

Figure 15 - Radiation Pattern For Small Aperture Monopole Antenna - (Harris Corporation)
(Vertical Polarization)

The EIRP, or effective isotropic radiated power, based on a 5 W transmitter, and 5 dB gain from this antenna, will produce about 12 dBW of power ($\text{EIRP} = \log(\text{Power}) \cdot 10 + \text{gain}$). The simple structure of this antenna should prove to be easy to deploy through the use of a collapsible graphite-epoxy constructed truss.

Another type of antenna, horizontally polarized, and thus designed for vertically incident sounding, is illustrated in Figure 16. This antenna's radiation pattern (Figure 17), is optimal in the vertical direction, especially at the low frequencies to be used on Mars. The height of the tower shown here is 6 meters. The element assembly at the top is 3.2 meters wide. For an input power of 10W and 8 db of gain, this antenna can provide an EIRP of 18 dBW.

An antenna could be designed combining both the elements of Figures 14 and 16 quite easily. Such an antenna would consist of a primary tower assembly truss, and upon remote command, deploy at the top of the tower the bow-tie element depending on whether horizontal polarization is required. Such a design would be useful for the Mars lander, in light of limited space available for multiple antennae.

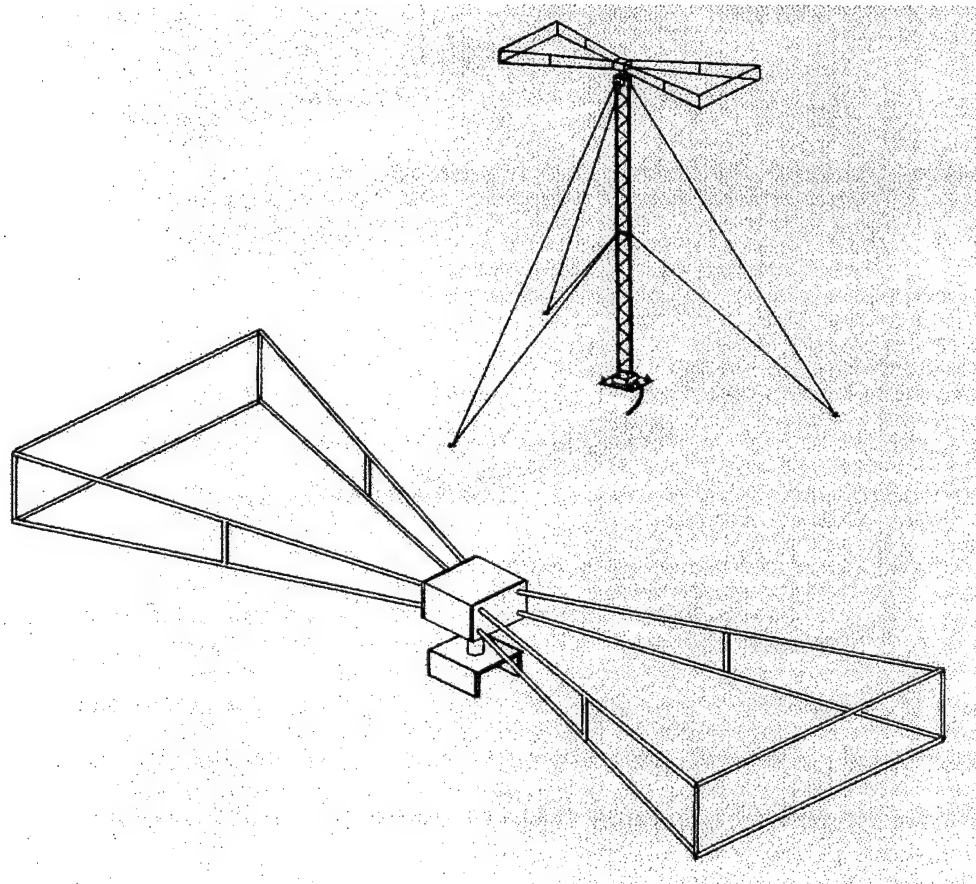
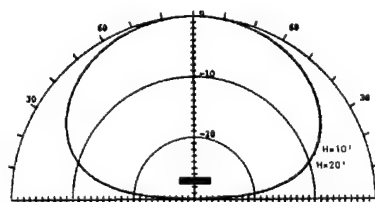
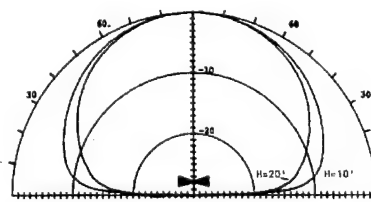


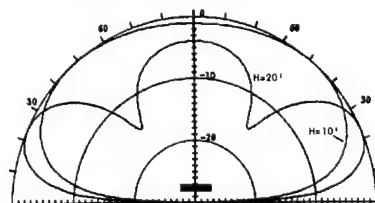
Figure 16 - Small Aperture Dipole Antenna - (Harris Corporation)



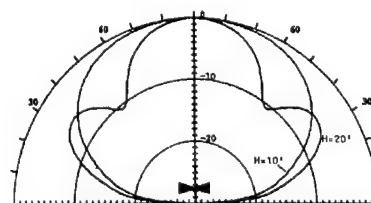
RF-1956 End View Elevation Pattern at 2 MHz.



RF-1956 Side View Elevation Pattern at 2 MHz.



RF-1956 End View Elevation Pattern at 30 MHz.



RF-1956 Side View Elevation Pattern at 30 MHz.

Figure 17 - Small Aperture Dipole Antenna Radiation Pattern - (Harris Corporation)

(Horizontal Polarization)

4.0 Design Implementation

The following sections will discuss at length the various considerations necessary for determining the component design for the Mars HF sounder. As is true for all spacecraft, whether remotely operated or astronauts onboard, redundancy must be factored into all design elements.

Due to the potentially harsh and unpredictable Mars environment, the sounder will have to be robust in design, including such elements as the antenna. Operation of the sounder will be at the highest level of autonomy possible, due to the impossibility of 'real time' operation from Earth - a radio command and acknowledgment signal would take approximately twenty minutes to travel a round-trip to Mars and back to Earth.

4.1 Critical Frequencies

Through analysis of the peak electron densities of the day and nighttime Martian ionosphere (Figures 2 and 18), one can also determine what is known as the critical frequency of the ionosphere. This is the highest frequency a vertically traveling radio wave will be reflected back to the surface. For a vertically incident

sounder, this essentially defines the frequency boundaries to be programmed into the sounder's transceiver unit. Given a daytime maximum electron density for Mars as $2 \times 10^5 \text{ cm}^{-3}$ (Verigin et al. 1991) and the formula: $f_c \text{ (in kHz)} = 9000 \bullet n_e^{1/2}$, this results in a critical frequency of 4000 kHz. For a nighttime peak of $5 \times 10^3 \text{ cm}^{-3}$, this results in a critical frequency of 636 kHz. In addition to the critical frequency, another important factor for consideration is the maximum usable frequency (MUF). This factor takes into account the incidence angle (I), or the angle at which the radio wave reflects upon reaching an ionospheric layer, (Elevation angle = $90 - \text{incidence angle}$). The angle will also depend on the transmitter site's latitudinal location and local elevation.

4.2 Maximum Usable Frequency

A MUF, or Maximum Usable Frequency, is defined as the highest frequency possible at a given time to provide reliable communications (McNamara, 1991). The MUF is calculated using both the critical frequency (f_c) and I (angle of incidence) ($\text{MUF} = f_c / \cos I$). On Mars, given the same electron peaks as in the critical frequency example, the MUF increases to up to 1 MHz for nighttime with an angle of incidence of 50 degrees. For daytime, the MUF increases to 6.2 MHz for an angle of incidence of 50 degrees.

Given these results for both critical and maximum usable frequencies, the design of the sounder's transceiver, specifically the portion of the spectrum it will sweep, can be better defined. Since by definition a vertically incident sounder will not change its antenna's elevation angle, the critical frequency parameters will be useful, while the MUF frequencies will only pertain to an obliquely incident sounder/receiver pair. Once an initial VI sounding is complete, a better estimate of useful frequencies for OI sounding will be possible. This system of adaptive design will limit the upper and lower bounds of the sounder, thus reducing its duty cycle period.

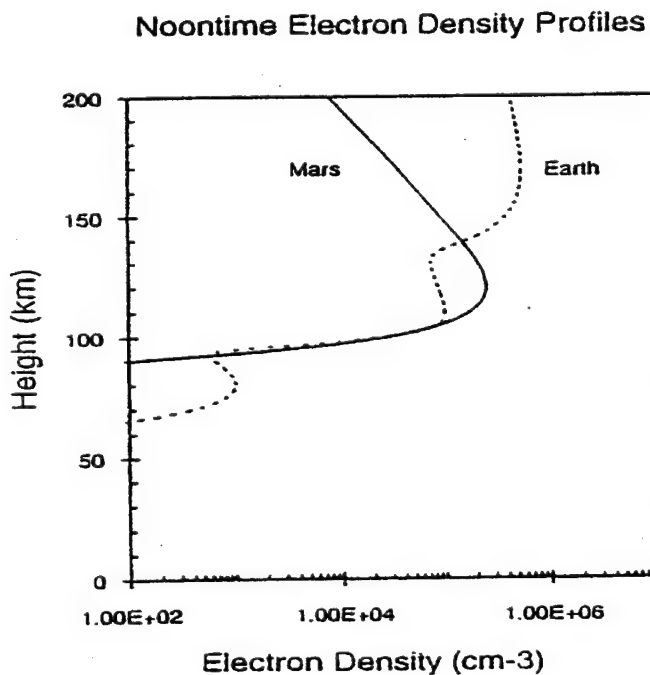


Figure 18 - Peak daytime electron peaks for Earth and Mars. (Fry, Yowell 1993)

4.3

Antenna Design

For both the oblique and vertically incident sounders, special consideration must be given to the design of the transmitting antenna. Figure 19 is an example of an obliquity factor chart for the E and F layers of the Earth's ionosphere. These plots assume an E layer reflection height of 100 km and an F layer reflection height of 300 km. The 'k' factor in the formula is a correction factor that takes into account the curvature of the Earth (1.1 under most conditions). From the figure, clearly the lower the elevation angle of the incident signal, the farther in distance it will travel.

If the obliquity factor is kept fixed by assuming a fixed circuit and the transmitting frequency is increased, the increasing frequencies will have to penetrate higher into the ionosphere in order for reflection to occur. Figure 20 illustrates how for a given circuit, higher frequencies leave the transmitting antenna at higher elevation angles. For this reason, it will be advantageous to design an antenna for the Mars lander that will accommodate the frequencies in the range from 500 kHz to 7 MHz over a distance of at least 1000 km. However, practicality of deployment options will force a compromise in antenna size and effectivity. A horizontal dipole design is therefore considered here for the Mars sounder.

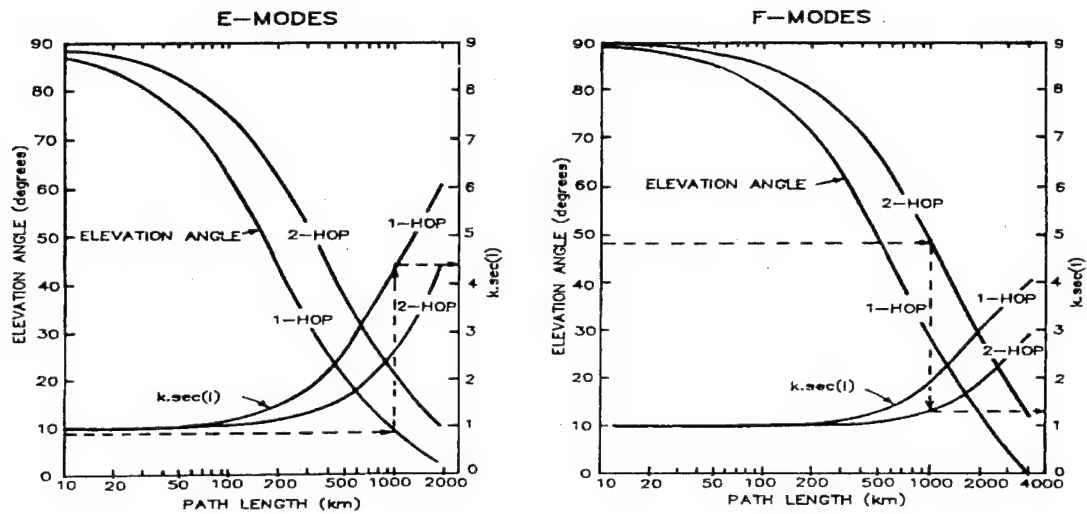


Figure 19 - Obliquity factor ($k \sec I$) and elevation angle as a function of circuit length for E and F layers. (McNamara, 1991)

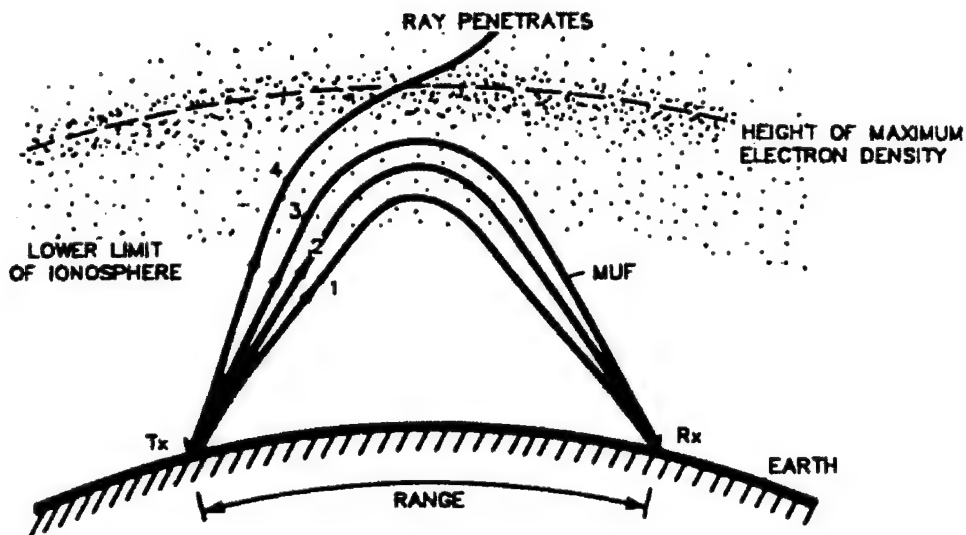


Figure 20 - Take-off angles of four different frequencies - and their propagation paths. (McNamara, 1991)

4.4

Horizontal Dipole Antennas

When one is selecting an antenna for transmission, power gain is an important factor. Gain is a function of both the antenna's directivity and efficiency. For a horizontally polarized antenna, the voltage reflection coefficient for a flat, perfectly conducting ground is -1, regardless of the angle of incidence. For an imperfect conducting surface, (e.g., Mars) the antenna pattern requires only a slight modification. The use of a horizontal vice vertically polarized antenna has the advantage of ignoring siting factors when considering directivity, and is thus advantageous when low signal launch angles are required. In our sounder design, we will use a factor of 0.3λ to determine the overall antenna length. If we assume the extreme case of transmission as low as a frequency of 500 kHz this would give us a length of over 700 meters - not a very practical option on Mars! If we consider the daytime MUF of 4 MHz, this would give an overall length of 23 meters, a more reasonable length. Deployment of such an antenna is possible through the use of a unique graphite-epoxy boom design, invented by engineers at NASA-JPL (Jet Propulsion Laboratory) and successfully tested on a 1985 Space Shuttle mission. On the Shuttle mission, a solar array some 30 meters tall was deployed and retracted out of the payload bay from a box only 30 cm tall. Such a design has the advantage of being retracted in the event of high winds

encountered during severe Martian dust storms. In the conceived lander design, this boom would also serve as the platform for the meteorological sensors.

4.5 In-Situ Data Transfer

For the operating scenario of several surface-based sounders, we must consider how the data from an ionogram will be sent to the 'central lander' for transmission back to earth. In conversation with Mr. Roy Sasselli, Chief Engineer from BR Communications, the question of ionogram transfer was discussed. In the current Chirpsounder design, an ionogram would take 30 kilobits of data to transfer digitally. If an ionogram was sent once an hour from each lander, this would be an excessive amount of data to send to earth; there would certainly be other experiments with even more data to transfer, not related to ionospheric sounding. If we assume that each lander would allocate a daily budget of data bandwidth, a complete set of 24 ionograms sent from each lander would not be practical.

To solve the data bandwidth problem, we can consider a compressed form of an ionogram for transmission. In conversation with Dr. John Goodman, SRI consultant, a terrestrial network known as Dynacast was discussed. This network of digitally linked sounders is now operating in support of the U.S. Navy. In lieu of sending entire ionograms back for processing, each sounder sends a compressed, autoscaled form of the ionogram, greatly reducing the 30 kb size of a

regular form. From Figure 13, we see that a typical ionogram contains lots of excess data. In fact, the only real data needed from an ionogram for 'operational' purposes, are the locations of the electron density peaks. Once this compressed ionogram is formed, its transmission via HF becomes much simpler, especially with today's advanced digital protocol systems.

4.5.1 Ionogram Sampling Periodicity

The limited duty cycle of the sounder, as well as power availability, dictates the need for careful selection of when and how often ionograms will be produced. As stated earlier, the daily 300 W of power available on the lander is the largest limiting factor. It is prudent therefore, to select time segments that would shift daily to eventually give a complete picture of the Martian ionosphere for diurnal conditions.

For example, if 5 ionograms are sampled daily, over a five day period, the entire 25 hour Martian day can be sampled. This could be accomplished by setting the sounder to sound at each of five consecutive hours. Each day, the time of the first sounding would shift by one hour forward. This method would be very useful not only for determination of sunrise, sunset effects, but also for determining dynamic changes as a result of solar flares, dust storms, or other unplanned events.

4.5.2 CLOVER HF Transmission Protocol

For many years, amateur radio operators have been using digital data communications over long distance paths. Morse code was really the first form of digital data transmission sent by radio. Over the years, amateur radio operators developed newer and better transmission modes, including radio teletype (RTTY), packet, and a new system known as CLOVER. CLOVER is a unique digital data transfer system, specifically designed for the HF spectrum (Henry and Petit, 1992). The CLOVER demodulation system dynamically and continuously measures key received signal to noise ratio, frequency dispersion, and time dispersion. Thus, its adaptive protocol can determine which of eight modulation modes, four data block lengths, and four Reed-Solomon error correcting codes to utilize for optimal data transmission.

The CLOVER system can vary the length of the data block it sends. Since block length and the number of Reed-Solomon correctable errors are proportional, longer blocks can correct more errors without requiring repeat transmissions. In cases where interference and ionospheric distortion are high, the error correction capability can become overloaded. To solve this problem, shorter block lengths can be sent. For average HF conditions, the CLOVER system can accommodate 200 to 300 bps throughput rates. For best HF conditions, this elevates to 500-600 bps. For the reduced data from our sounders, the CLOVER

option would work very well for data transfer from peripheral landers to the 'mother' lander, for transfer back to Earth.

4.6 Follow-On Experiments

In addition to the methodology presented here for a surface-based ionospheric sounder, an alternate experiment may later be implemented which would involve the use of an orbiting satellite, simultaneously communicating with a ground based sounder. This is known as transionospheric sounding; for many years this method has been successfully used for study of Earth's ionosphere. Two methods will be presented here, direct transionospheric sounding and inverse transionospheric sounding.

By using radio frequencies at slightly above the plasma frequency, one can create a complete top and bottomside picture of the ionosphere. The satellite would contain an onboard beacon that would simultaneously transmit two radio pulses directly to a ground receiver. Such a satellite was orbited by the Soviet Union in the late 1970's - - Intercosmos 19 (Danilkin, 1994).

The first pulse of 100 μ s duration is at a constant frequency, just above the plasma frequency. The second pulse of 133 μ s duration transmits at a varying frequency, changing from pulse to pulse. After both pulses have passed

through the ionosphere, the pulse transmitted at the lower frequency will be received later than the pulse transmitted at the higher frequency. By measuring this time delay, the ground based receiver can create an ionogram. The top schematic in Figure 21 shows that the satellite contains two transmitters (ref. boxes 4, 5), one receiver (9), signal generator (1) and modulator (2). Telemetry pulses are sent simultaneously with sounding pulses. The propagation time for both depends on the height of the satellite, the satellite location angle and ionospheric conditions.

Inverse transionospheric sounding involves using a high power ground based transmitter synchronized to timing pulses that are transmitted from the satellite. As shown in Figure 22, timing pulses from the satellite signal a ground based ionosonde (boxes 2 and 11) to begin operating in synch with the satellite's ionosonde. The transmitter (11) transmits a vertical signal which is received at the satellite and then retransmitted (6) to another ground station, along with the ionograms (4 and 5) computed onboard the satellite.

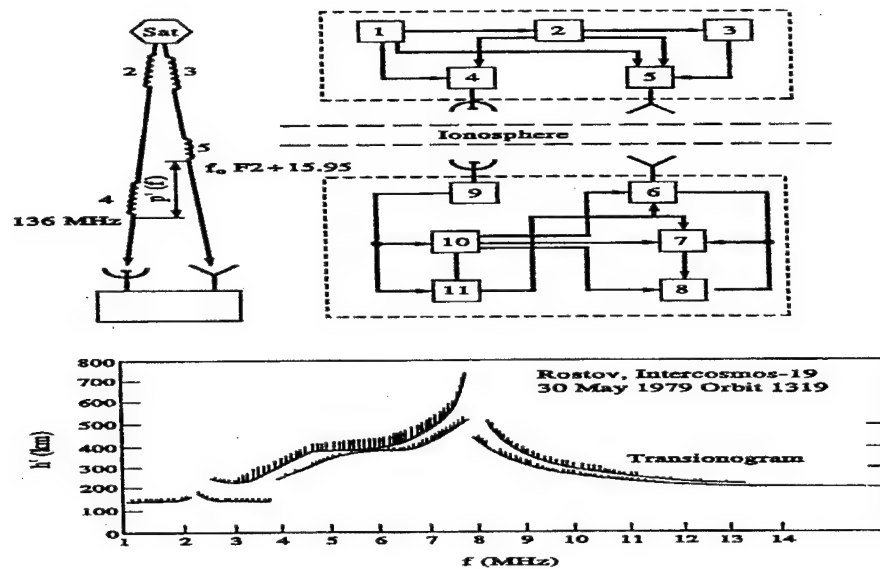


Figure 21 - Direct transionospheric radio sounding schematic and actual transionogram (Danilkin, 1994)

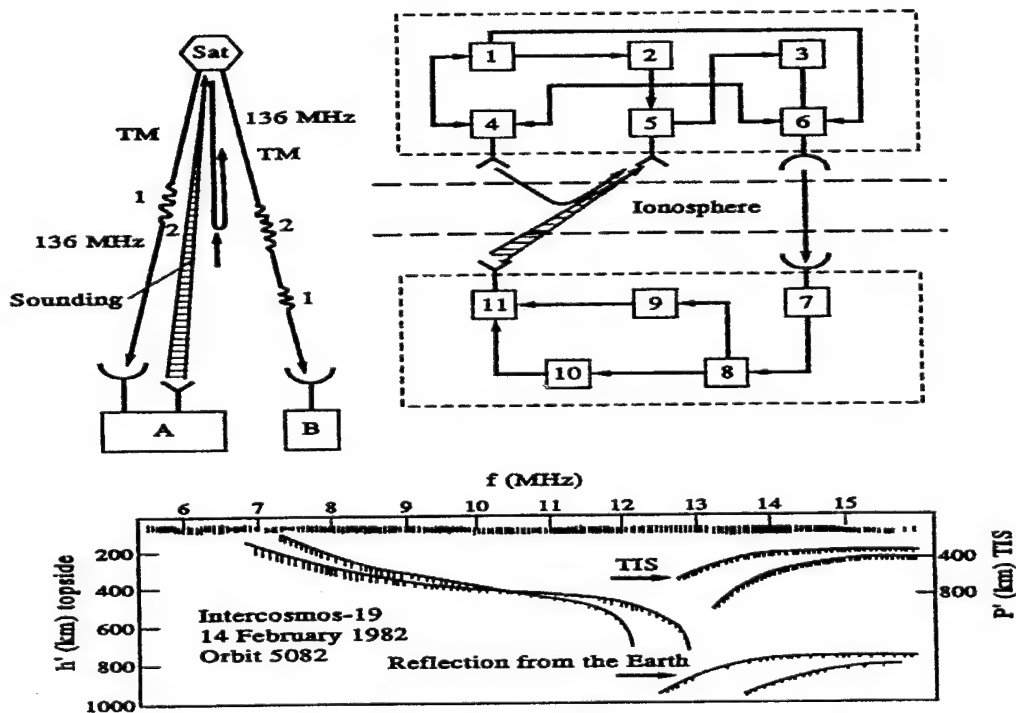


Figure 22 - Inverse transionospheric radiosounding - schematic, and transionogram (Danilkin, 1994)

5.0 Conclusions and Recommendations

5.1 Summary

A review of the literature regarding past Mariner, Viking and other missions to the planet Mars reveals the existence of an ionospheric layer in the Martian atmosphere. Based on the electron density profiles seen in these missions, as well as from simulation models, it was determined that the best choice of frequencies for a surface-based Martian ionospheric sounder is in the range of 1 to 15 MHz.

Based on the required lander power margins, an operating power consumption range of 10 - 15 W was chosen; this range makes the choice of a Chirpsounder unit very appropriate. Combining this factor with the chosen sounding frequencies, a horizontal dipole antenna providing vertical polarization was chosen for the sounder. This antenna, combined with a deployable boom assembly, would work well in light of the limited space afforded by the lander. In anticipation of overall data requirements for each lander, a method of data compression will be used to reduce the amount of time necessary for the sounding experiment to send ionograms to the central lander. In addition, a unique method of digital error correction coding will reduce negative effects of propagation phenomena.

5.2 Conclusions

On the basis of this feasibility and design study for the sounder experiment, the following conclusions are drawn:

1. Existing data from previous missions, verifying the existence of a Martian ionosphere, is a prime justification for sending an ionospheric sounder to the Martian surface.

2. A surface based ionospheric sounder can be integrated successfully into existing templates for future Martian robotic landers.

5.3 Recommendations

Based on the observations and assumptions made during this analysis, the following recommendations are made for further study:

1. Earth-based tests of antenna designs and low power ionosondes would be useful prior to their selection for the Mars lander. These tests should occur at high latitude polar regions, since their electron density profiles would be the closest terrestrial analogue to the Mars environment.

2. Earth-based tests of HF data compression techniques would improve the efficiency of transferring ionograms from Mars to Earth.

3. An effort to discover unusual HF propagation modes can be an additional element of the sounder experiment. Both oblique and vertically incident soundings may reveal the existence of "Sporadic-E" type behavior during dust storms, trans-equatorial propagation, "Spread-F" phenomena, and meteor burst communication. By carefully selecting landing sites, and time of operation, these phenomena may be revealed.

4. In addition to sky wave propagation, ground wave propagation should be investigated as another mode of long distance communication on Mars. This will depend heavily on the conductivity factor of Martian soil.

5.4 Denouement

The ionospheric sounder, or ionosonde can trace its roots back to the first decade of this century. To this day, after many design improvements thanks to digital technology, the sounder is still an integral part of the science of aeronomy, providing crucial information to users of the HF spectrum around the world.

With advances in digital and microelectronic technology, the capability of integrating a sounder into a space and power constrained spacecraft is now a reality. The Chirpsounder has opened the door to the aeronomic study of another planet.

From an operational perspective, the potential for HF over-the-horizon communications as a viable primary system, will allow for the design of less expensive robotic missions, with the potential for data gathering over a much wider area of the planet.

The planet Mars presents the first environment away from Earth where an ionospheric sounder could provide valuable new scientific information regarding another ionosphere. In order to comprehend the dynamic processes that shaped and continue to shape the Martian atmosphere, an understanding of its ionosphere is essential.

A valuable by-product of the information gleaned from bottomside soundings of the Martian ionosphere will be the ability to plan future missions using a backup capability of over-the-horizon communications without the need of an orbiting satellite. This redundancy may prove to be the factor that determines mission failure or mission success.

APPENDIX

A.1 Ionospheric Layers

The atmospheric layer known as the ionosphere is formed when extreme ultraviolet (EUV) light from the sun strips electrons from the neutral atoms of the Earth's atmosphere. The strength and intensity of the EUV light from the sun is not constant at all wavelengths but is much stronger at the wavelength of the emitting atom, (eg. Hydrogen). The density of the atoms which are photoionized in this process decreases as altitude increases. Also, the intensity of the EUV light producing the photoionization decreases towards lower altitudes since the light is absorbed by the upper layers of the atmosphere. The net result of these opposing effects is the production of a layer of electron with a maximum electron density at a given altitude and lower electron densities above and below this level. Because the intensity of EUV radiation varies with wavelength, and there is a large variety of atoms and molecules in the atmosphere, the ionosphere contains up to four different layers at different altitudes.

The first layer of the ionosphere discovered by E.V. Appleton was noted to exist at an altitude of 100 km, and was called the E layer. The D layer exists at heights of 50 to 90 km, and the F layer covers 150 to 600 km.

During local daylight in the summer season, the F layer splits into two layers, F₁ and F₂; thus the Earth's ionosphere consists of the D, E, F₁, and F₂ layers. At night, when photoionization ceases, recombination eliminates most of the free electrons left in the ionosphere, and removes most of the layers. The only surviving layer is the F₂ layer, and this layer provides for nighttime long distance HF propagation (McNamara, 1991).

A.2 Chapman Layers

In order to better interpret the radio occultation data of the Martian ionosphere, one must understand Chapman layer theory. A Chapman layer is a model of an ionosphere where photoionization described by a constant cross section is balanced by local recombination described by a constant cross section, so that it is a photochemical equilibrium ionosphere. In an "ideal" Chapman layer, the neutral atmosphere density and constant scale height H , are presumed to be independent of solar zenith angle. All solar zenith angle variations of the ionosphere are then determined by the path length of radiation absorbed by the atmosphere. The theory presumes that the atmosphere is planar, so that the solar zenith angle variations result purely from the varying angle of incidence of the ionizing radiation .

Two basic characteristics of the ideal Chapman layer are the $\cos^{1/2}\theta$ dependence of the electron density at the peak of the altitude profile on

solar zenith angle θ , and the dependence of the peak altitude h_m on solar zenith angle of $h_m(\theta) = h_m(0) + H \ln \sec \theta$ which implies that the peak altitude increases as one approaches the terminator.

Ionospheres fail to be described by Chapman layers for a number of reasons. First, many ionospheres experience some internal transport of ionization by both diffusion and convection. This redistribution produces electron density profiles that depend not only on the local production and loss rates, but on pressure gradients and the frequencies of collisions between ions and neutrals, ions and ions, and ions and electrons. In addition, the recombination coefficient actually varies with the electron temperature, and thus with altitude. The uppermost regions of ionospheres that closely interact with the solar wind can experience unusual ion production from mechanisms like impact ionization and charge exchange of neutrals with solar wind protons. They are also subject to additional nonradiative sources of heating that affect the topside altitude profiles of the plasma density by altering the plasma pressure gradients, the effects of exterior and interior magnetic pressure, and losses by solar wind “scavenging”. These phenomena are of interest because they tell us what controls a planetary ionosphere and how factors like the solar wind can influence a planet’s ionosphere and atmosphere (Zhang et al. 1990). Figure A1 shows a typical Chapman profile of zenith angle (y axis) vs. electron density (x axis).

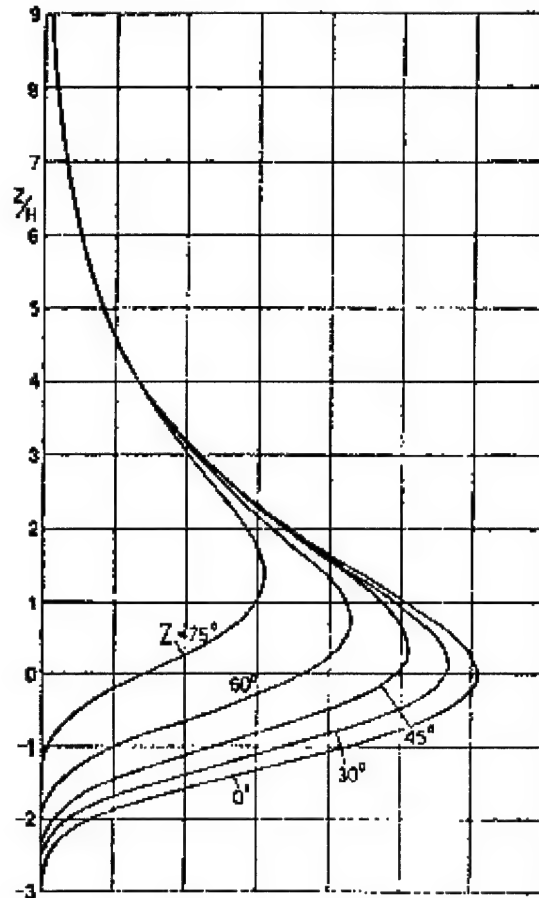


Figure A1 - Distribution of electron density vs. solar zenith angle (McNamara, 1991)

A.3

Solar Cycle

The ionosphere's dependence on EUV radiation for photoionization is a very important relationship. In fact, in order to study the ionosphere and make valid predictions for radio propagation links, one must understand the sun's 11 year sunspot cycle.

A major source of EUV light from the sun are sunspots. These dark splotches on the sun form in large groups every eleven years. Individual spots can form at any time, but the 11 year "solar maximum" period coincides with the most active periods of photoionization in the F layers of the ionosphere.

The unfortunate down side of the solar maximum period is that along with increased amounts of sunspots being produced, the sun is also more apt to create a solar flare. These flares are a sudden release of magnetic energy, usually from an active sunspot region. The X-rays that are produced from this flare can have a very negative effect on ionospheric radio propagation. If the flare is of sufficient severity, the X-rays it produces may penetrate down to the ionosphere's D layer, causing much higher levels of photoionization and electron density in this layer. This leads to maximum absorption of all HF signals being sent into the ionosphere from the surface, and is known as shortwave fadeout. This condition, depending on the flare, may cause a total loss of reflective capability in the ionosphere for up to two hours (McNamara, 1991).

A.4 Martian Ionogram Model

The following Matlab program was written in order to provide a simulation of an ionogram produced from a surfaced based sounder on the

Martian surface. The formulas used in this program are based on the following equation for virtual height (Davies, 1990): $h' = h_0 + \sum \mu' \Delta h_i$. The virtual, or group height as a function of frequency is one of the most useful of ionospheric characteristics. An ionogram yields the virtual height based on electron density profile, the plasma frequency, and the radio frequency being transmitted during the sounding.

The formula for μ' , the group refractive index is (Davis, 1990): $\mu' \mu = \mu^2 + 2/D [1 - \mu^2 - X^2 + (1-\mu^2)(1-X^2) Y_L^2 / A]$.

Since we are ignoring collisions in our Mars model, the entire fraction on the right side of the equation equals zero. We are therefore left with $\mu' = \mu + 2 / 2(1-X) [1 - \mu^2 X^2]$. Since $\mu^2 = 1 - X$, we then solve again for μ' and get for our result: $\mu' = 1 / (1 - X)^{1/2}$ (since $\mu' \mu = 1$ when collisions are ignored).

When calculating virtual height, special precautions must be taken near the level of reflection where μ' approaches infinity. In order to accomplish this, a check is written into the program to verify that the ratio of $1 / (1-X)^{1/2}$ does not approach infinity. In addition the results produced from this program were compared to those attained through the following virtual height approximations given by Davies: 1) $h' = h_0 + \pi / 2\beta [1 +/-(f_H / f)^2]^{1/2} (f +/ - 1/4 f_H)$

$$2) h' = 2H [\tanh^{-1} \mu_0 -/+ Y / 2(1 +/ - Y) \mu_0]$$

When +/- or -/+ are used, the numerator's sign goes together, denoting a z or longitudinal wave, while the denominator's sign goes together, denoting an x or transverse wave.

Coding For Ionogram Simulation Program

<u>Code</u>	<u>Comments</u>
flow=0.05e6; fhigh=15e6;	Define range of sounding frequencies (50 kHz - 15 MHz).

delta=0.025; df=0.1e6;	Define increment to limit 'X' value for μ calculation. Define increment of sounding frequency step.

base=110e3; top=135e3;	Define bottom height of ionosphere. Define top height of ionosphere.
dl=5e3; dh=500;	Define height of of altitude layers. Define separation of altitude layers.

```
freq=[flow:df:fhigh];
```

```
h1=[0:dh:base-dh];
```

Determine overall electron density profile.

```
h2=[base:dh:top-dh];
```

```
h=[h1,h2];
```

```
ne=zeros(size(1:round(base/dh)));
```

Set electron density to zero from surface to bottom
of ionosphere

```
mupri=zeros(size(1:length(h)));
```

```
x=zeros(size(1:length(h)));
```

```
if 110e3<=h<135e3
```

Set electron density profile

```
ne=(10e6/25)*(h-110e3);
```

```
if 135e3<=h<=160e3
```

```
ne=(10e6) - (10e6/25)*(h-135e3);
```

```
vh=zeros(size(1:length(freq)));
```

```
fn = sqrt(80.5*[ne]);
```

Determine plasma frequency

```
for j=1:length(freq),
```

```
for i=1:length(h),
```

```
x(i)=(fn(i)^2)/(freq(j)^2);
```

Compute 'X' from Appleton's Equation.

```
if x(i)>(1-delta)
```

```
mupri(i)=sqrt(1-x(i));
```

Compute μ' at reflection layer.

```
else
```

mupri(i)=1/sqrt(1-x(i));	Compute μ' below reflection layer
end	
if (freq(j)>=fn(i))	Ensure plasma frequency does not exceed
	radio frequency
vh(j)=vh(j)+dh*mupri(i);	Compute virtual height
vh(j);	
end	
end	
end	
end	
end	
plot(freq,vh)	
print marsgram	

Bibliography

- Agarwal, D.C., "Electromagnetic Wave Propagation In the Martian Ionosphere", Journal of the Institution of Telecommunications Engineers, 18 : 26-28 (1972).
- Brandt, J.C. and M.B. McElroy. The Atmospheres of Venus and Mars. New York: Gordon and Breach Science Publishers, Inc., 1968.
- Chen, R.H., et al., "The Martian Ionosphere In Light of the Viking Observations", Journal of Geophysical Research, 83: 3871-3876 (1978).
- Chicarro, A.F. et al., "Marsnet Phase-A Study Report", ESA Publication SCI (93)2: 99-103 1993
- Cravens, T.E. . "Ionospheric Models For Venus and Mars", Geophysical Monograph, 66: 277-288 (1991).
- Davies, Kenneth. Ionospheric Radio. London: Peter Peregrinus Ltd., 1990.
- Fox, J.L. et al. "The Martian Thermosphere/Ionosphere at High and Low Solar Activities", Advances in Space Research, 17 : 203-208 (1996).
- Fry, C.D., and R.J. Yowell. "HF Radio On Mars", Communications Quarterly, 4 : 13-23 (1994).
- Goodman, John M. HF Communications: Science and Technology. New York: Van Nostrand Reinhold, 1992.
- Goodman, John M. Private Communication, (1996).
- Hantsch, M.H. and S.J. Bauer. "Solar Control of the Mars Ionosphere", Planetary and Space Science, 38 : 539-542 (1990).
- Hargreaves, J. K. The Solar-Terrestrial Environment. New York: Cambridge University Press, 1992.
- Henry, Bill and Petit, Ray. "HF Radio Data Communication: CW to CLOVER", Communications Quarterly, 2: 20-34 (1992).
- Kazantsev, A.N. "Comparison of Parameters of the Mars Ionosphere According to Mariners 4, 6 and 7 Measurements and to Calculations of Radiowave Absorption", Proceedings - Space Research XI: (1971).
- Klimov, S.I., et al. "On the Use of a Mobile Surface Radar to Study the Atmosphere and Ionosphere of Mars", Advances In Space Research, 10: 35-38 (1990).

- Kolosov, M.A., et al. "Investigation of Radiowave Propagation in the Solar System", IEEE Transactions on Antennas and Propagation, AP-27: 18-21 (1979).
- Luhmann, J.G. and L.H. Bruce. "Near-Mars Space", Reviews of Geophysics, 29: 121-140 (1991).
- Luhmann, J.G. "Outstanding Problems in Mars Aeronomy", Advances in Space Research, 15: 143-157 (1995).
- McCormick, P.T. and R.C. Whitten. "On the Effect of Electron-Neutral Particle Collisions Upon the Refraction of High-Frequency Radio Waves by the Lower Atmosphere and Ionosphere of Mars", Planetary and Space Science, 21: 881-883 (1973).
- McNamara, Leo F. . The Ionosphere: Communications, Surveillance and Direction Finding. Malabar: Krieger Publishing, 1991.
- Michael, W.H. Jr., et al. "The Viking Radio Science Investigations", Journal of Geophysical Research, 82: 4293-4295 (1977)
- Ratcliffe, J.A. . An Introduction to the Ionosphere and Magnetosphere. New York: Cambridge University Press, 1992.
- Saselli, Roy. Private Communication, (1996).
- Savich, N.A. and V.A. Samovol. "The Night Time Ionosphere of Mars from Mars 4 and Mars 5 Dual-Frequency Radio Occultation Measurements", Proceedings - Space Research XVI: 1009-1011 (1976).
- Shinagawa, H. and T.E. Cravens. "A One-Dimensional Multispecies Magnetohydrodynamic Model of the Dayside Ionosphere of Mars", Journal of Geophysical Research 94: 6506-6516 (1989).
- Stewart, A.J. and W.B. Hanson. "Mars' Upper Atmosphere: Mean and Variations", Advances In Space Research 2: 87-101 (1982).
- Verigin, M.I., et al. "On The Possible Source of the Ionization In the Nighttime Martian Ionosphere", Journal of Geophysical Research 96: 19307-19313 (1991).
- Winchester, C. and D. Rees. "Numerical Models of the Martian Coupled Thermosphere and Ionosphere", Advances In Space Research 15: 51-68 (1995).
- Zhang, M.H.G., et al. "A Post-Pioneer Venus Reassessment of the Martian Dayside Ionosphere as Observed by Radio Occultation Methods", Journal of Geophysical Research 95: 14829-14839 (1990).
- Zhang, M.H.G., et al. "An Observational Study of the Nightside Ionospheres of Mars and Venus with Radio Occultation Methods", Journal of Geophysical Research 95: 17095-17102 (1990).

REPORT DOCUMENTATION PAGE

Form Approved
OMB No. 0704-0188

Public reporting burden for this collection of information is estimated to average 1 hour per response, including the time for reviewing instructions, searching existing data sources, gathering and maintaining the data needed, and completing and reviewing the collection of information. Send comments regarding this burden estimate or any other aspect of this collection of information, including suggestions for reducing this burden, to Washington Headquarters Services, Directorate for Information Operations and Reports, 1215 Jefferson Davis Highway, Suite 1204, Arlington, VA 22202-4302, and to the Office of Management and Budget, Paperwork Reduction Project (0704-0188), Washington, DC 20503.

1. AGENCY USE ONLY (Leave blank)		2. REPORT DATE June 1996	3. REPORT TYPE AND DATES COVERED Master's Thesis	
4. TITLE AND SUBTITLE INVESTIGATION OF RADIO WAVE PROPAGATION IN THE MARTIAN IONOSPHERE UTILIZING HF SOUNDING TECHNIQUES			5. FUNDING NUMBERS	
6. AUTHOR(S) Robert J. Yowell, Civilian NASA				
7. PERFORMING ORGANIZATION NAME(S) AND ADDRESS(ES) Air Force Institute of Technology, WPAFB OH 45433-7765			8. PERFORMING ORGANIZATION REPORT NUMBER AFIT/GE/ENG/96J-01	
9. SPONSORING / MONITORING AGENCY NAME(S) AND ADDRESS(ES) Exploration Physics International 586-3 Nashua St., Suite 222 Milford, NH 03055-4992			10. SPONSORING / MONITORING AGENCY REPORT NUMBER	
11. SUPPLEMENTARY NOTES				
12a. DISTRIBUTION / AVAILABILITY STATEMENT Approved for public release; distribution unlimited			12b. DISTRIBUTION CODE	
13. ABSTRACT (Maximum 200 words) This thesis presents a preliminary design of an ionospheric sounder to be carried aboard one or more of NASA's Mars Surveyor landers. Past Russian and American probes have indicated the existence of an ionosphere, but none of these missions remotely sensed this atmospheric layer from the surface. The rationale for utilizing a surface-based Martian ionospheric sounder is discussed. Based on NASA's choice of launch vehicle and power source, a low-weight, low-powered Chirpsounder using a horizontally-polarized dipole antenna is recommended for the sounder experiment. The sounder experiment should be conducted for at least one Martian year, in order to investigate significant changes in radio propagation during seasonal transitions. Specific data compression techniques are suggested in order to reduce the quantity of data transferred from each sounder. The Appendix presents an overview of Earth's ionospheric structure and solar cycle effects. Finally, a Matlab software model of a hypothetical ionogram as measured from the Martian surface is presented.				
14. SUBJECT TERMS Ionosphere, Sounding, Mars, Planetary Atmospheres			15. NUMBER OF PAGES 74	
			16. PRICE CODE	
17. SECURITY CLASSIFICATION OF REPORT Unclassified	18. SECURITY CLASSIFICATION OF THIS PAGE Unclassified	19. SECURITY CLASSIFICATION OF ABSTRACT Unclassified	20. LIMITATION OF ABSTRACT UL	

GENERAL INSTRUCTIONS FOR COMPLETING SF 298

The Report Documentation Page (RDP) is used in announcing and cataloging reports. It is important that this information be consistent with the rest of the report, particularly the cover and title page. Instructions for filling in each block of the form follow. It is important to *stay within the lines* to meet *optical scanning requirements*.

Block 1. Agency Use Only (Leave blank).

Block 2. Report Date. Full publication date including day, month, and year, if available (e.g. 1 Jan 88). Must cite at least the year.

Block 3. Type of Report and Dates Covered. State whether report is interim, final, etc. If applicable, enter inclusive report dates (e.g. 10 Jun 87 - 30 Jun 88).

Block 4. Title and Subtitle. A title is taken from the part of the report that provides the most meaningful and complete information. When a report is prepared in more than one volume, repeat the primary title, add volume number, and include subtitle for the specific volume. On classified documents enter the title classification in parentheses.

Block 5. Funding Numbers. To include contract and grant numbers; may include program element number(s), project number(s), task number(s), and work unit number(s). Use the following labels:

C - Contract	PR - Project
G - Grant	TA - Task
PE - Program Element	WU - Work Unit Accession No.

Block 6. Author(s). Name(s) of person(s) responsible for writing the report, performing the research, or credited with the content of the report. If editor or compiler, this should follow the name(s).

Block 7. Performing Organization Name(s) and Address(es). Self-explanatory.

Block 8. Performing Organization Report Number. Enter the unique alphanumeric report number(s) assigned by the organization performing the report.

Block 9. Sponsoring/Monitoring Agency Name(s) and Address(es). Self-explanatory.

Block 10. Sponsoring/Monitoring Agency Report Number. (If known)

Block 11. Supplementary Notes. Enter information not included elsewhere such as: Prepared in cooperation with...; Trans. of...; To be published in.... When a report is revised, include a statement whether the new report supersedes or supplements the older report.

Block 12a. Distribution/Availability Statement. Denotes public availability or limitations. Cite any availability to the public. Enter additional limitations or special markings in all capitals (e.g. NOFORN, REL, ITAR).

DOD - See DoDD 5230.24, "Distribution Statements on Technical Documents."

DOE - See authorities.

NASA - See Handbook NHB 2200.2.

NTIS - Leave blank.

Block 12b. Distribution Code.

DOD - Leave blank.

DOE - Enter DOE distribution categories from the Standard Distribution for Unclassified Scientific and Technical Reports.

NASA - Leave blank.

NTIS - Leave blank.

Block 13. Abstract. Include a brief (*Maximum 200 words*) factual summary of the most significant information contained in the report.

Block 14. Subject Terms. Keywords or phrases identifying major subjects in the report.

Block 15. Number of Pages. Enter the total number of pages.

Block 16. Price Code. Enter appropriate price code (*NTIS only*).

Blocks 17. - 19. Security Classifications. Self-explanatory. Enter U.S. Security Classification in accordance with U.S. Security Regulations (i.e., UNCLASSIFIED). If form contains classified information, stamp classification on the top and bottom of the page.

Block 20. Limitation of Abstract. This block must be completed to assign a limitation to the abstract. Enter either UL (unlimited) or SAR (same as report). An entry in this block is necessary if the abstract is to be limited. If blank, the abstract is assumed to be unlimited.